SNP, 518C>G (A173G, **2* allele), was found at a frequency of 0.594. As for *1A10*, eight SNPs were detected. Among them, two polymorphisms, 4G>A (A2T) and 200A>G (E67G), were novel (Figure 2). Previously reported SNPs 177G>A (M59I, **2* allele) and 605C>T (T202I, **3* allele) were both found at a 0.010 frequency. Seven polymorphisms were detected in *1A9*, and two of them, −126_−118 T9>T11 and 422C>G (S141C), were novel (Figure 3). The SNPs 726T>G (Y242X, **4* allele) and 766G>A (D256N, **5* allele) were found at frequencies of 0.003 and 0.010, respectively. In this study, the known insertion, −126_−118 T9>T10 (**22* allele), was also detected at a 0.666 frequency. A total of nine SNPs including two novel ones (−70G>A, and 726T>C (Y242Y)) were detected in *1A7* (Figure 3). The known nonsynonymous SNPs, 387T>G (N129K), 391C>A and 392G>A (R131K: the SNPs at 391 and 392 are completely associated), and 622T>C (W208R), were also detected at frequencies of 0.350, 0.350, and 0.219, respectively. In *1A3*, 10 SNPs were detected, and only 46C>T (L16L) was novel. The known nonsynonymous SNPs,

Gene			*UGT1A8*								*UGT1A10*								
Position[a]			34332	34781	34863	34974	35028	35067	35307		53108	53279	53302	53707	53795	54091	54163	54255	
Nucleotide change[b]			69 T>C	518 C>G	600 C>T	711 A>C	765 A>G	804 T>C	IVS1 +189 G>A		4 G>A	177 G>A	200 A>G	605 C>T	693 C>T	IVS1 +134 G>C	IVS1 +206 A>G	IVS1 +298 G>C	
Amino acid change			A23A[c]	A173G	A200A[c]	T237T[c]	Y255T[c]	N268N[c]			A2T	M59I	E67G	T202I	A231A[c]				
Functional change				no change								no change		reduced					Frequency
Reference			novel	[8]	novel	rs 1126805[d]	rs 1042605[d]	Pharm GKB data base[e]	Pharm GKB data base[e]		novel	[11]	novel	[11]	rs 17863767[d]	rs 1901814[d]	Pharm GKB data base[e]	Pharm GKB data base[e]	
Marker allele				*2			*1a				*2T	*2	*67G	*3					
Haplotype[f]	Block	Segments																	
	*1 (*1*1)	*1a	*1b*1a															0.311	
		*1b	*1c*1a															0.051	
		*1c	*1a*1c															0.015	0.390
		*1d	*1d*1a															0.010	
		*1e	*1b*1b															0.003	
	*8 (*2*1)	*8a	*2a*1a															0.492	
		*8b	*2a*1b															0.084	0.584
		*8c	*2b*1a															0.008	
	*18 (*2*2)	*18a	*2a*2a															0.010	0.010
	*IV (*1*3)	*IVa7	*1a*3a															0.005	
		*IVb	*1a*3b															0.003	0.010
		*IVc	*1e*3a															0.003	
	*V (*1*2T)	*Va	*1c*2T															0.003	0.003
	*VI (*1*67G)	*VIa	*1b*67G															0.003	0.003
SNP frequency			0.008	0.594	0.003	0.054	0.026	0.010	0.594		0.003	0.010	0.003	0.010	0.026	0.094	0.026	0.026	

Figure 2 SNPs and haplotypes of *UGT1A8* and *1A10* (*Block 8/10*) in a Japanese population. [a]Position on AF297093.1. [b]A of the initiation codon in each gene segment is numbered 1. For intron SNPs, their positions were numbered from the nearest exon. [c]No amino-acid change. [d]dbSNP number in the National Center for Biotechnology Information. [e]The SNPs included in the PharmGKB database (http://www.pharmgkb.org/). [f]The haplotypes are described as numbers plus alphabetical letters. The prediction of rare haplotypes that were inferred from only one subject (frequency was 0.003) is sometimes inaccurate.

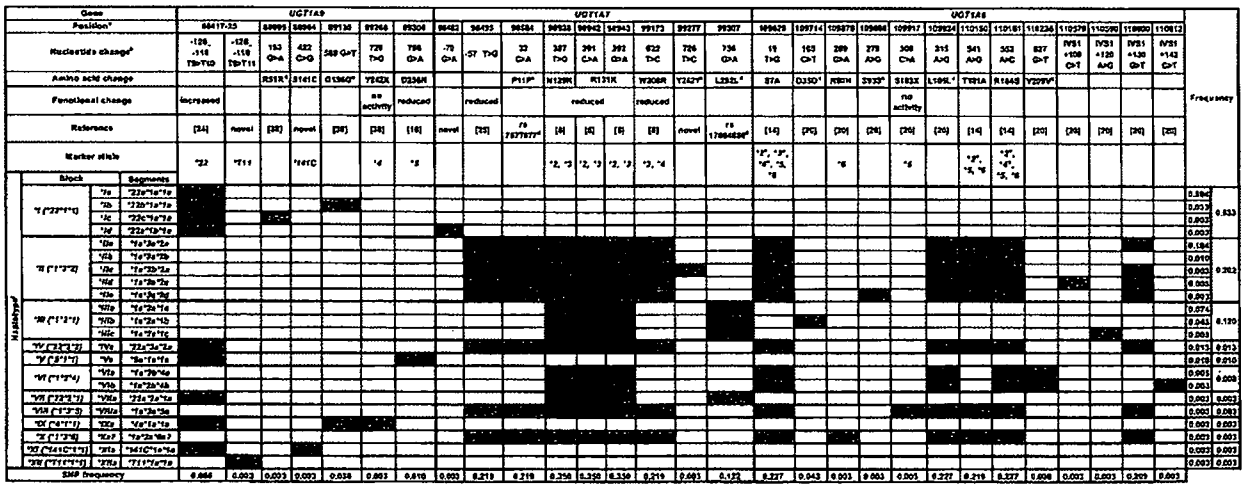

Figure 3 SNPs and haplotypes of *UGT1A9*, *1A7*, and *1A6* (*Block 9/6*) in a Japanese population. [a]Position on AF297093.1. [b]A of the initiation codon in each gene segment is numbered 1. For intron SNPs, their positions were numbered from the nearest exon. [c]No amino-acid change. [d]dbSNP number in the National Center for Biotechnology Information. [e]The haplotype numbering of *UGT1A6* basically followed the numbering by Nagar *et al*.[14] [f]The haplotypes are described as numbers plus alphabetical letters. The prediction of rare haplotypes that were inferred from only one subject (frequency was 0.003) is sometimes inaccurate.

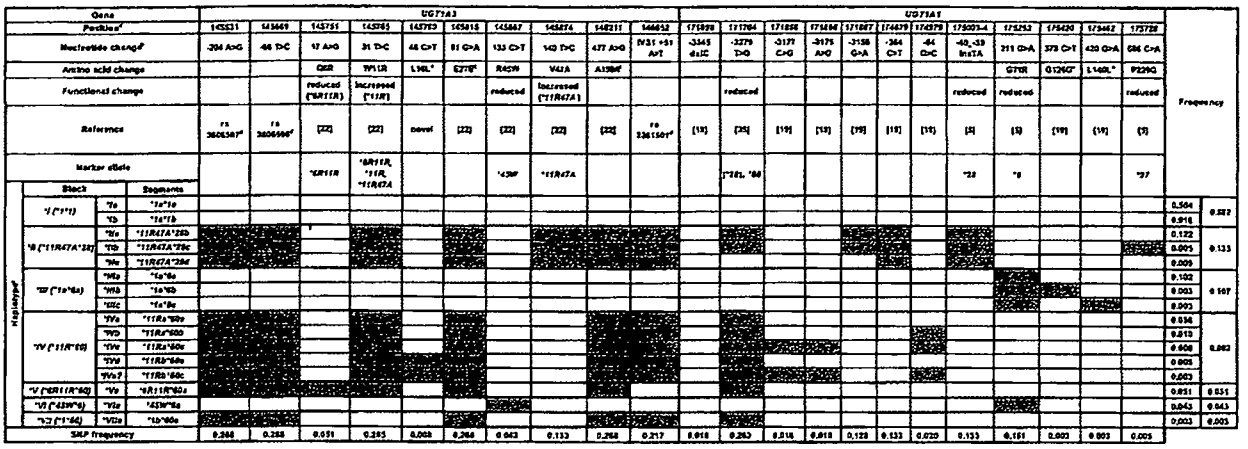

Figure 4 SNPs and haplotypes of *UGT1A3* and *1A1* (*Block 3/1*) in a Japanese population. [a]Position on AF297093.1. [b]A of the initiation codon in each gene segment is numbered 1. For intron SNPs, their positions were numbered from the nearest exon. [c]No amino-acid change. [d]dbSNP number in the National Center for Biotechnology Information. [e]The haplotypes are described as numbers plus alphabetical letters. The prediction of rare haplotypes that were inferred from only one subject (frequency was 0.003) is sometimes inaccurate.

17A>G (Q6R), 31T>C (W11R), 133C>T (R45W), and 140T>C (V47A), were detected at frequencies of 0.051, 0.265, 0.043, and 0.133, respectively (Figure 4).

LD analysis

Next, pairwise LD analysis was performed for the *UGT1A* genes using the polymorphisms detected in this study (*1A8*, *1A10*, *1A9*, *1A7*, and *1A3*) and previous studies (*1A6*, *1A4*, *1A1*, and common exons 2–5)[19–21] from the same 196 subjects, and the values for rho square (r^2), chi square (χ^2), and $|D'|$ were obtained. Variations found in only one subject were excluded from the analysis. Since the data for r^2 and χ^2 values were almost equivalent, only the data for r^2 is depicted in Figure 5. Several close linkages within each segment were seen between the variations of the *1A8*, *1A10*, *1A7*, and *1A3* gene segments, as seen in the *1A6*, *1A4*, and *1A1* segments and common exons that were previously analyzed. Furthermore, strong linkages were also observed across the segments, especially between *1A8* and *1A10*, among *1A9*, *1A7*, and *1A6*, and between *1A3* and *1A1*, where approximately 19, 35.5, 10, 11, 26, 10.5, and 29.5 kb separate *1A10* from *1A8*, *1A9* from *1A10*, *1A7* from *1A9*, *1A6* from *1A7*, *1A4* from *1A6*, *1A3* from *1A4*, and *1A1* from *1A3*, respectively. Thus, the region from *1A8* to *1A1* was divided into four LD blocks: *Block 8/10* (*1A8* and *1A10*), *Block 9/6* (*1A9*, *1A7*, and *1A6*), *Block 4* (*1A4*), and *Block 3/1* (*1A3* and *1A1*). The data from the $|D'|$ values supported this block partitioning (data not shown). In addition, a few exceptional strong linkages (over 0.7 for r^2) beyond the LD blocks were also observed. The perfect linkage ($r^2=1$) was detected between *1A10* 177G>A (M59I) and *1A9* 766G>A (D256N), and between *1A4* IVS1+101G>T and *1A1* 686C>A (P229Q). A strong LD ($r^2=0.95$) was also shown between *1A8* 711A>C (T237T) and *1A3* 17A>G (Q6R). In addition, *1A7* 756G>A (L252L) was strongly linked with *1A4* −219C>T, −163G>A, 142T>G (L48V), 448T>C (L150L), 804G>A (P268P), and IVS1+43C>T ($r^2=0.78$ or greater). The other linkages were less than 0.67 for r^2.

Haplotype analysis

Next, the haplotypes for *Block 8/10*, *Block 9/6*, and *Block 3/1* were analyzed. The haplotypes of *Block 4*, consisting of the *1A4* segment,[21] and *Block C*, covering common exons 2–5 (*Block 2* in a previous paper[19]), have already been reported. The block haplotypes were tentatively named with Roman numerals plus small alphabetical letters. The haplotypes were also estimated for each gene segment (segment haplotypes), where a group of haplotypes without amino-acid changes was defined as **1*.

As for *Block 8/10*, consisting of the two segments *1A8* and *1A10*, six haplotypes were first unambiguously assigned by the presence of homozygous SNPs at all sites (**Ia*, **Ib*, **IIa*, and **IIb*) or a heterozygous SNP at only one site (**IIc* and **IIIa*). We separately estimated the diplotype configuration (a combination of haplotypes) for each subject by LDSUPPORT software. The diplotype configurations of 184 subjects were inferred with a probability greater than 0.96, and the remaining diplotypes (12 subjects) had a probability greater than 0.54. The haplotype inferred in the diplotypes with low probabilities were described with a question mark in Figure 2 (i.e., **IVa?*). There were eight additionally inferred haplotypes. The block haplotypes were also described in the form of segment haplotype (*1A8* haplotype-*1A10* haplotype) combinations in Figure 2: in the *1A8* segment, the segment haplotype bearing the nonsynonymous A173G (**2* allele) was named **2*; in *1A10*, the haplotypes bearing M59I (**2* allele), T202I (**3* allele), A2T, and E67G were named **2*, **3*, **2T*, and **67G*, respectively. The most frequent block haplotype (segment haplotype combination in parenthesis) was **IIa* (**2a*1a*) (frequency: 0.492), followed by **Ia* (**1b*1a*) (0.311), **IIb* (**2a*1b*) (0.084), and **Ib* (**1c*1a*) (0.051). The frequencies of other block haplotypes were less than 0.05.

Figure 5 Linkage disequilibrium (LD) analysis of *UGT1A* SNPs. Pairwise LD is expressed as r^2 (from 0 to 1) by a 10-graded blue color for the polymorphisms ($n=2$ or greater) in *1A8, 1A10, 1A9, 1A7, 1A6, 1A4, 1A3, 1A1*, and common exons 2–5 located in the same order on the chromosome. The denser color represents the higher linkage. *Block C*: the same as *Block 2* in the previous paper, and the nucleotide positions of polymorphisms in the exons 2–5 are numbered as in *UGT1A1*.[19] UTR: untranslated region.

It is noteworthy that the low-activity *1A10* haplotype **3* was completely linked with the *1A8*1* haplotype (*Block 8/10 *IV*).

Regarding *Block 9/6* (*1A9-1A7-1A6*), 14 haplotypes were first unambiguously assigned by homozygous SNPs at all sites (**Ia, *Ib, *IIa*, and **IIIa*) or a heterozygous SNP at only one site (**Ic, *Id, *IIc, *IId, *IIIb, *IVa, *Va, *VIIIa, *XIa*, and **XIIa*). Additionally, eight haplotypes (**IIb, *IIe, *IIIc, *VIa, *VIb, *VIIa, *IXa*, and **Xa?*) were inferred, and diplotype configurations of 191 subjects were inferred with a 1.00 probability by the software. The haplotype inferred in the diplotype with a low probability was **Xa?* (Figure 3). The block haplotypes were also described as combinations of segment haplotypes (*1A9* haplotype-*1A7* haplotype-*1A6* haplotype) in Figure 3: in the *1A9* segment, the segment haplotype bearing Y242X (**4* allele), D256N (**5* allele), −126_−118 T9>T10 (**22* allele), −126_−118 T9>T11, or S141C were named **4,*5, *22, *T11*, or **141C*, respectively; in the *1A7* segment, the haplotype bearing N129K/R131K (**2* allele) was named **2*, and the haplotype bearing N129K/R131K/W208R (**3* allele) was named **3*; in *1A6*, the haplotypes bearing S7A/T181A/R184S (**2* allele), S7A/R184S (**4* allele), S7A/S103X/T181A/R184S (**5* allele), and S7A/R90H/T181A/R184S (**6* allele) were named **2, *4, *5,*

and *6*, respectively, as described previously.[20] The most frequent haplotype of *Block 9/6* was **Ia* (**22a*1a*1a*) (0.594), followed by **IIa* (**1a*3a*2a*) (0.184), and **IIIa* (**1a*2a*1a*) (0.074) (Figure 3). The frequencies of the other haplotypes were under 0.05. Notably, most (97.6%) of the high-activity segment haplotype *1A9*22* was linked with *1A7*1* and *1A6*1* (*Block 9/6 *I*). The *1A7* low-activity haplotype **3* was mostly linked (97.7%) with *1A6*2* haplotype (**II* and **IVa* in Figure 3).

Regarding *Block 3/1* (*1A3-1A1*), six haplotypes were first unambiguously assigned by the presence of homozygous SNPs at all sites (**Ia*, **IIa*, **IIIa*, and **Va*) or a heterozygous SNP at only one site (**Ib* and **VIa*). The diplotype configurations of 188 subjects were inferred with a 1.00 probability. The additionally inferred haplotypes were **IIb*, **IIc*, **IIIb*, **IIIc*, **IVa–*IVe?*, and **VIIa*. The haplotype **IVe?* was inferred with a low probability (Figure 4). The combinations of segment haplotypes (*1A3* haplotype-*1A1* haplotype) were also described in Figure 4: in *1A3*, the group bearing the nonsynonymous variations Q6R/W11R, W11R, R45W, and W11R/V47A were named the **6R11R*, **11R*, **45W*, and **11R47A* haplotypes, respectively;[22] in *1A1*, the haplotypes bearing G71R (**6* allele), −40_−39 insTA (**28* allele with or without **60* allele), and −3279T>G (**60* allele without **28* allele) were named the **6*, **28*, and **60* haplotype groups as described previously.[19] The most frequent haplotype of *Block 3/1* was **Ia* (**1a*1a*) (frequency: 0.564), followed by **IIa* (**11R47A*28b*) (0.122), **IIIa* (**1a*6a*) (0.102), **IVa* (**11Ra*60a*) (0.056), and **Va* (**6R11R*60a*) (0.051). The frequencies of the other block haplotypes were less than 0.05. It is noteworthy that the high-activity segment haplotype *1A3*11R47A* was completely linked with the low-activity haplotype *1A1*28* (*Block 3/1 *II*). The low-activity haplotype *1A1*6* was mostly linked (71.3%) with the *1A3*1* haplotype (**III*). The high-activity *1A3*11R* haplotype was perfectly linked with the low-activity *1A1*60* haplotype (**IV*).

Finally, no statistically significant differences in haplotype frequencies were found between the subjects with the different disease types in *Block 8/10*, *Block 9/6*, and *Block3/1* ($P \geqslant 0.05$ by χ^2 test or Fisher's exact test).

Genotyping and haplotype analysis across the LD blocks

A typing method was developed and additional 105 Japanese subjects (16 arrhythmic patients and 89 cancer patients) were genotyped, where direct sequencing (for nine polymorphisms in the *1A9* 5′-flanking region and *1A4*) and pyrosequencing (for the rest of the polymorphisms) were used for detection of 41 polymorphisms (see Materials and methods and the Table 1 legend) with (potentially) functional importance. The frequencies from 301 subjects in total are described in Table 1. Again, all the allele frequencies were in Hardy–Weinberg equilibrium, and statistically significant differences were not observed in any of the allelic frequencies between the two disease types ($P \geqslant 0.05$ by χ^2 test or Fisher's exact test). Almost the same LD map as in Figure 5 was obtained between the 41 tagged variations (data not shown), indicating the robustness of our block partitioning. It is noteworthy that the known variation *1A1* 1456T>G (Y486D, **7* allele) was newly found in one subject (frequency: 0.002).

Several reports have shown that some polymorphisms in *1A9*, *1A7*, *1A6*, and *1A1* were closely linked,[17,18] and we also observed several weak linkages beyond the LD blocks (see Figure 5). Therefore, the block-haplotype combinations (whole complex haplotypes) were analyzed among *Block 8/10*, *Block 9/6*, *Block 4*, *Block 3/1*, and *Block C* (common exons 2–5) by LDSUPPORT software utilizing the polymorphisms. In *1A4* (*Block 4*), the haplotypes bearing L48V (**3* allele) and R11W (**4* allele) were named **3* and **4*, respectively, as described previously.[21] Polymorphisms found at a frequency less than 0.010, and subjects with these polymorphisms were excluded in this analysis. When *Block 8/10* or *Block C* was included in the analysis, the whole-complex haplotypes were highly complicated (data not shown). However, if *Block 8/10* and *Block C* were excluded, the diplotype configurations of 278 subjects were inferred with a probability greater than 0.91 (mostly>0.95) using the 18 tagged polymorphisms (see Figure 6 legend for polymorphisms). The haplotypes covering *Block 9/6*, *Block 4*, and *Block 3/1* are summarized in Figure 6. Again, we did not find any statistically significant differences in frequencies of haplotypes covering *Block 9/6*, *Block 4* and *Block 3/1* between the subjects with the different disease types ($P \geqslant 0.05$ by χ^2 test or Fisher's exact test). The region from *1A9* to *1A1* is approximately 90 kb length. Since the 18 variations were used for haplotyping, the number of inferred haplotype combinations (only 26) is unexpectedly small compared to the theoretical ones (Figure 6).

Several functionally important linkages were found across the blocks. *Block 9/6 *VI* (*1A9*1-1A7*2-1A6*4*) and *Block 3/1 *IIb* (*1A3*11R47A-1A1*28c* containing the **60*, **28*, and **27* alleles) were perfectly linked (6/6 cases). Most of the *1A1*6*-containing haplotypes (*Block 3/1 *III* and **VI*) (69/85 cases) were associated with *Block 4* (*1A4*) **1* and *Block 9/6 *II* (harboring *1A7*3* and *1A6*2*). The *1A1*60*-harboring haplotypes (*Block 3/1 *IV* and **V*) were very closely linked with *Block 9/6 *III* (harboring *1A7*2*) and *Block 4 *3* (59/71 cases of *1A1*60*-harboring haplotypes). Most of *Block 3/1 *VI* (*1A3*45W-1A1*6*) (25/26 cases) was associated with *Block 9/6 *II* (*1A9*1-1A7*3-1A6*2*), and *Block 4 *4* was perfectly linked (4/4 cases) with both *Block 3/1 *VI* and *Block 9/6 *II*.

In addition, we found that *Block 8/10 *IV* (containing the low-activity allele *1A10*3* (T202I)) was strongly linked with *Block 9/6 *III* (*1A9*1-1A7*2-1A6*1*), *1A4*3*, and *Block 3/1 *IV* (*1A3*11R-1A1*60*) (4/5 cases of *Block 8/10 *IV*, data not shown). *Block 3/1 *V* (harboring *1A3*6R11R* and *1A1*60a*) was perfectly linked with *Block C *IB* (25/25 cases of *Block 3/1 *V*, data not shown).

Discussion

Previously, we have reported the genetic variations of *UGT1A6*, *1A4*, *1A1* segments and common exons 2–5 found in 196 Japanese subjects.[19–21] In this study, we first directly

Table 1 Frequencies of variations in the *UGT1A* gene complex detected in 301 Japanese subjects

Location	*Nucleotide change*		*Amino-acid change*	*Number of subjects*			*Frequency*
				Wild type	*Heterozygote*	*Homozygote*	
1A8 Ex1	518[a]	C>G	A173G	48	145	108	0.600
1A10 Ex1	4[a]	G>A	A2T	300	1	0	0.002
	177[a]	G>A	M59I	297	4	0	0.007
	200[a]	A>G	E67G	300	1	0	0.002
	605[a]	C>T	T202I	295	6	0	0.010
1A9 5′-Flank	−126 to −118	T9>T10		34	130	136	0.668
		T9>T11			1	0	0.002
1A9 Ex1	422[a]	C>G	S141C	300	1	0	0.002
	726[a]	T>G	Y242X	300	1	0	0.002
	766[a]	G>A	D256N	297	4	0	0.007
1A7 Ex1	387[a]	T>G	N129K	128	135	38	0.350
	391[a]	C>A		128	135	38	0.350
	392[a]	G>A	R131K	128	135	38	0.350
	622[a]	T>C	W208R	186	101	14	0.214
1A6 Ex1	19[a]	T>G	S7A	180	106	15	0.226
	269[a]	G>A	R90H	300	1	0	0.002
	308[a]	C>A	S103X	300	1	0	0.002
	541[a]	A>G	T181A	186	101	14	0.214
	552[a]	A>C	R184S	180	106	15	0.226
1A4 Ex1	31	C>T	R11W	295	6	0	0.010
	127	delA	43fsX22[b]	300	1	0	0.002
	142	T>G	L48V	229	66	6	0.130
	175	delG	59fsX6[b]	299	2	0	0.003
	271	C>T	R91C	300	1	0	0.002
	325	A>G	R109G	299	2	0	0.003
1A4 3′-Flank	IVS+1	G>T		300	1	0	0.002
1A3 Ex1	17[a]	A>G	Q6R	276	24	1	0.043
	31[a]	T>C	W11R	167	111	23	0.261
	133[a]	C>T	R45W	274	26	1	0.047
	140[a]	T>C	V47A	228	69	4	0.128
1A1 5′-Flank	−3279[a]	T>G		167	110	24	0.262
	−40 to −39[a]	insTA		227	70	4	0.130
1A1 Ex1	211[a]	G>A	G71R	217	76	8	0.153
	247[a]	T>C	F83L	301	0	0	0.000
	686[a]	C>A	P229Q	295	6	0	0.010
1A Ex4	1091[a,c]	C>T	P364L	298	3	0	0.005
1A Ex5	1456[a,c]	T>G	Y486D	300	1	0	0.002
	1598[a,c]	A>C	H533P	300	1	0	0.002
1A 3′-UTR	1813[a,c]	C>T		236	63	2	0.111
	1941[a,c]	C>G		236	63	2	0.111
	2042[a,c]	C>G		236	63	2	0.111

[a]In all, 105 subjects were genotyped by pyrosequencing.
[b]43fsX22 represents frameshift from codon 43 resulting in the termination at the 22nd codon, codon 65. The same meaning for 59fsX6.
[c]The positions in *UGT1A1* were used.

Block 9/6				Block 4	Block 3/1			Number of combination	Frequency
UGT1A9	*UGT1A7*	*UGT1A6*		*UGT1A4*	*UGT1A3*	*UGT1A1*			
*22	*1	*1	*I	*1	*1	*1	*I	323	0.581
*1	*3	*2	*II	*1	*1	*1	*I	3	0.005
*1	*2	*1	*III	*1	*1	*1	*I	3	0.005
*22	*1	*1	*I	*3	*1	*1	*I	1	0.002
*22	*3	*2	*IV	*1	*1	*1	*I	1	0.002
*1	*3	*2	*II	*1	*1	*6	*III	48	0.086
*22	*3	*2	*IV	*1	*1	*6	*III	7	0.013
*22	*1	*1	*I	*1	*1	*6	*III	3	0.005
*1	*2	*1	*III	*1	*1	*6	*III	1	0.002
*1	*3	*2	*II	*1	*45W	*6	*VI	21	0.038
*1	*3	*2	*II	*4	*45W	*6	*VI	4	0.007
*22	*1	*1	*I	*1	*45W	*6	*VI	1	0.002
*22	*1	*1	*I	*1	*11R47A	*28b	*IIa	30	0.054
*1	*3	*2	*II	*1	*11R47A	*28b	*IIa	30	0.054
*1	*3	*2	*II	*3	*11R47A	*28b	*IIa	1	0.002
*1	*2	*4	*VI	*1	*11R47A	*28c	*IIb	6	0.011
*22	*1	*1	*I	*1	*11R47A	*28d	*IIc	1	0.002
*1	*3	*2	*II	*1	*11R47A	*28d	*IIc	1	0.002
*1	*2	*1	*III	*3	*11R	*60	*IV	36	0.065
*22	*1	*1	*I	*3	*11R	*60	*IV	3	0.005
*1	*3	*2	*II	*3	*11R	*60	*IV	3	0.005
*1	*2	*1	*III	*1	*11R	*60	*IV	3	0.005
*22	*1	*1	*I	*1	*11R	*60	*IV	1	0.002
*1	*2	*1	*III	*3	*6R11R	*60	*V	23	0.041
*1	*2	*1	*III	*1	*6R11R	*60	*V	1	0.002
*22	*2	*1	*VII	*3	*6R11R	*60	*V	1	0.002
								556	1.000

Figure 6 Combinations of *Block 9/6*, *Block 4*, and *Block 3/1* haplotypes in a Japanese population. The used variations were *UGT1A9* −126_−118 T9>T10, *1A7* 387T>G, 391C>A, 392G>A and 622T>C, *1A6* 19T>G, 541A>G and 552A>C, *1A4* 31C>T and 142T>G, *1A3* 17A>G, 31T>C, 133C>T and 140T>C, and *1A1* −3279T>G, −40_−39 insTA, 211G>A and 686C>A. In *1A4* (*Block 4*), the haplotypes bearing L48V (**3* allele), and R11W (**4* allele) were named **3* and **4*, respectively.

sequenced *1A8*, *1A10*, *1A9*, *1A7*, and *1A3* using genomic DNA from the same Japanese subjects and detected 7, 8, 7, 9, and 10 genetic polymorphisms, respectively (Figures 2–4). Two and one novel nonsynonymous SNPs were found in *1A10* (4G>A, A2T; 200A>G, E67G) and *1A9* (422C>G, S141C), respectively. As for 1A9 S141C, our preliminary results have shown that this amino-acid substitution reduces the enzymatic activity against 7-hydroxy-4-trifluoromethylcoumarin *in vitro* (Jinno *et al.*, unpublished data). Since the guanine base at position +4 is important for translation initiation,[23] *1A10* 4G>A might decrease the translation rate. Moreover, the luciferase-reporter activity of *1A9* −126_−118 T10 (*1A9*22* allele) was reported to increase 2.6-fold as compared to that of *1A9* −126_−118 T9.[24] Therefore, the novel variation *1A9* −126_−118 T9>T11 may also affect transcriptional activity. Further studies are needed to ascertain these possibilities. Recently, *1A7* −57G was reported to reduce the luciferase activity by 70% of the wild-type −57T.[25] While this SNP is linked with either *1A7*3* (129K/131K/208R) or **4* (208R) in Germans, our study showed that −57G was completely linked with *1A7*3* due to the absence of *1A7*4* in Japanese.

For the *1A8* alleles, only **1* and **2* were detected. Our segment haplotypes **1a*, **1b*, and **2a* correspond to alleles **1a*, **1*, and **2*, respectively, in a previous study on Americans.[8] The frequencies obtained in the United States,[8] 0.282, 0.551, and 0.145, for **1a*, **1*, and **2*, respectively, are different from those obtained in this study, 0.023, 0.316, and 0.587 for **1a*, **1b*, and **2a*, respectively. The allele frequency of *1A9* −126_−118 T9>T10 (**22* allele) in our data (0.666) was similar to that reported previously in Japanese (0.60), but higher than those in Caucasians (0.39) and African-Americans (0.44).[24] For *1A7*, the frequencies of **1*, **2* (129K/131K), and **3* (129K/131K/208R) haplotypes were 0.651, 0.130, and 0.219, respectively. Our data are comparable to the previous data for a Japanese population,[26] but not to those on Caucasians (0.355, 0.280, and 0.365) and Egyptians (0.420, 0.200, and 0.380).[17] As for *1A3*, the frequencies of the haplotypes **1*, **11R*, **6R11R*, **11R47A*, and **45W* were 0.692, 0.082, 0.051, 0.133, and 0.043, respectively. These are similar to the previous data obtained from the Japanese.[22]

Recently, linkages among the SNPs in *1A9*, *1A7*, *1A6*, and *1A1* have been reported in Americans.[18] By our LD analysis, strong linkages were shown between the SNPs in *1A8* and *1A10*, among those in *1A9*, *1A7*, and *1A6*, and also between those in *1A3* and *1A1*. Moreover, this is the first report on the haplotype analysis using high-density SNPs for the entire *UGT1A* complex. By block haplotyping, several close linkages between the segmental haplotypes were observed: between the *1A8*1* and *1A10*3* haplotypes in *Block 8/10*; between the *1A7*3* and *1A6*2* in *Block 9/6*; between the *1A3*11R47A* and *1A1*28* and between the *1A3*11R* and *1A1*60* haplotypes in *Block 3/1*. Carlini *et al.*[18] reported that

1A7 low-activity alleles (*1A7*2* and **3*) were perfectly linked to *1A9*1* in Americans (including Caucasians (83%) and African-American (14%)). Also in this study, most (95.6%) of the *1A7*2* or **3* alleles were linked to the *1A9*1* allele in Japanese (Figure 3).

We conducted additional typing of 105 subjects by pyrosequencing and direct sequencing, and confirmed the presence of several functionally important haplotype combinations beyond the blocks (Figure 6). In Americans (including Caucasians (83%) and African-American (14%)),[18] Caucasians, and Egyptians,[17] 75, 78, and 57%, respectively, of *1A7*3* were associated with the *1A1*28* allele, though only the **28* allele was genotyped in *1A1* in these analysis. In our more intensive analysis, most of the *1A7*3* haplotype was associated with either the *1A1*28b* haplotype (having *1A1*60* and **28* alleles) (26.1% of the *1A7*3* haplotype) or the *1A1*6* haplotype (67.2% of *UGT1A7*3*). Thus, different profiles for the linkage of *1A7*3* with the *1A1* polymorphisms between the Caucasians and Japanese reflect the facts that the frequency of the *1A1*6* haplotype in the Asian populations was relatively high, and that the *1A1*28* and **6* alleles were mutually exclusive.[19] In fact, linkage between *1A1*6* and *1A7*3* alleles was recently suggested in Taiwanese.[27] Innocenti *et al.* reported the three most common *1A9-1A1* haplotype combinations were *1A9*22-1A1*1* (36.4%), *1A9*1-1A1*28b* (28.0%), and *1A9*1-1A1*1* (18.6%) for Caucasians, and *1A9*22-1A1*1* (45.3%), *1A9*1-1A1*60* (22.3%), and *1A9*1-1A1*6* (12.7%) for Asians.[28] In this study for Japanese, *1A9*22-1A1*1*, *1A9*1-1A1*60*, and *1A9*1-1A1*6* (58.5, 11.9, and 13.3%, respectively) were also the most common three combinations. Furthermore, we revealed that most (98.2%) of the *1A1*1* haplotype was linked with *1A9*22*, and 87.1% of *1A1*6*, 100% of *1A1*28c*, and 93.0% of *1A1*60* were associated with *1A9*1*. Collectively, haplotype combinations are suggested to be different between Caucasians and Asians. In addition, several interesting linkages were found between the segmental haplotypes as shown in the Results. For example, the segment haplotypes *1A6*4* (S7A/R184S) and *1A1*28c* were strongly linked in Japanese subjects.

These linkages might be crucial for the metabolism of a certain drug for which two or more UGT1A isoforms significantly contribute to its metabolism. In fact, multiple UGT isoforms are involved in glucuronidation of several compounds, for example SN-38,[7,29] estrogens and their metabolites (estron, estradiol, 2-hydroxyestrone, and others),[30,31] and arachidonic acid and its metabolites.[32,33] UGT1A1, 1A9, and 1A7 play important roles in SN-38 glucuronidation.[7,29] The *1A1*60*, **28b*, and **6* haplotypes are associated with reduced UGT1A1 activity to SN-38.[15,19,34,35] Since the *1A9* high-activity (high transcription) haplotype **22* was dominant in Japanese (0.666), *1A9*1* can be considered (relative to **22*) as a low-activity haplotype. The *1A7*3*, but not **2*, haplotype has a reduced glucuronidation activity (by 59%) to SN-38.[7] A more recent report has shown that UGT1A10 is also responsible for SN-38 glucuronidation,[36] and that the *1A10 *3* (T202I) is a low-activity allele.[11] We found that the *Block 8/10 *IV* haplotype (harboring *1A10*3*) was closely linked with *Block 9/6 *III* (harboring *1A9*1*) and *Block 3/1 *IV* (harboring *1A1*60*). Furthermore, most of *Block 9/6 *II* (harboring *1A9*1* and *1A7*3*) were estimated to be linked with *Block 3/1 *III* or **VI* (having *1A1*6*), or *Block 3/1 *IIa* (having *1A1*28b*). Though the functional significance of 1A10 T202I toward SN-38 is currently unknown, it is possible that the concurrently reduced activities of UGT1A10, 1A9, 1A7, and 1A1 may influence SN-38 glucuronidation.

Arachidonic acid and its metabolites prostaglandins were conjugated with UGT1A1, 1A3, 1A9, 1A10, and 2B7.[33] UGT1A1, 1A3, and 1A4 also had catalytic activities toward a hydroxylated metabolite of arachidonic acid, 12- and 15-hydroxyeicosatetraenoic acid.[32] Furthermore, glucuronidation of leucotriene B4, another arachidonic acid metabolite that mediates the inflammation process, can be catalyzed by UGT1A1, 1A3, 1A8, and 2B7.[32] Thus, co-occurrence of the functionally less active haplotypes (such as *Block 9/6 *II* (including *1A9*1*)-*Block 3/1 *VI* (harboring *1A3*45W* and *1A1*6*)), might cooperatively influence the metabolism of several important compounds in the arachidonic acid cascade.

Since plural UGT isoforms are often involved in the glucuronidation of 'one' compound, co-occurrence of the functionally less active haplotypes in the entire *UGT1A* gene complex needs to be carefully considered in studies on the association of genetic polymorphisms with pharmacokinetic parameters and clinical and epidemiologic data. Our findings would provide fundamental and useful information for genotyping or haplotyping of *UGT1As* in the Japanese and probably other Asian populations.

Materials and methods

Human genomic DNA samples

The 301 Japanese subjects consisted of 124 arrhythmic patients, who were administered β-blockers, and 177 cancer patients, who were administered irinotecan. Genomic DNA was extracted directly from blood leukocytes. The ethical review boards of the National Cancer Center, the National Cardiovascular Center, and the National Institute of Health Sciences approved this study. Written informed consent was obtained from all patients.

Polymerase chain reaction (PCR) conditions for DNA sequencing

First, the fragments were amplified from genomic DNA (150 ng) using 2.5 U of Z-Taq (Takara Bio Inc., Shiga, Japan) with 0.2 μM primers (see '1st amplification' in Table 2 for primer sequences). The exon-1's of *UGT1A8* and *1A10* were simultaneously amplified by mixed primers for each gene, and those of *1A9* and *1A7* were amplified as one fragment. The primer sequences for the 1st amplification of *1A10* were described previously.[37] The first PCR conditions consisted of 30 cycles of 98°C for 5 s, 55°C for 5 s, and 72°C for 190 s. Then, each exon 1 was amplified by Ex-Taq (0.625 U) (Takara Bio Inc.) using the first PCR products as templates with the 2nd amplification primers (0.2 μM) that were designed in the introns (see '2nd amplification' in Table 2 for primer

Table 2 Primers for amplification and sequencing of exon-1's in *UGT1A8, 1A7, 1A3,* and 5'-flanking region of *1A9*

	Direction	*Gene*	*Primer name*	*Sequences*
1st amplification	Forward	*1A8*	UGT1A8ZF	5'-GTGGCTGGTACTCATTTTTCC-3'
	Reverse		UGT1A8ZR	5'-CTTCCAAACCCAACATCTCTAA-3'
	Forward	*1A9-7*	UGT1A9-7ZF	5'-TCTTGATTGTCCTCCATTGAGT-3'
	Reverse		UGT1A9-7ZR	5'-ACCAAGCAACCATACTCATAGG-3'
2nd amplification	Forward	*1A8*	UGT1A8-1stF	5'-AGAATGTGGAAGTAGAGCGG-3'
	Reverse		UGT1A8-1stR	5'-TTAGCAAAAAAGGAAAGTTCAA-3'
	Forward	*1A9* 5'-Flank	UGT1A9pro-248F1st	5'-TTGAGACAGAGTCGTGCTGTT-3'
	Reverse		UGT1A9pro-608R1st	5'-GCAAAGCCACAGGTCAGC-3'
	Forward	*1A7*	UGT1A71stF	5'-AAATGAATGAATAAGTACACGCC-3'
	Reverse		UGT1A71stR	5'-GGAAGTTTCATTTCTTACTGTGG-3'
	Forward	*1A3*	UGT1A3-1stF	5'-GTGAGCACAGGGTCAGACGTGT-3'
	Reverse		UGT1A3-1stR	5'-TTACAAACATTCGTGTCTACTT-3'
Sequencing	Forward	*1A8* Exon1	UGT1A8Ex1Fseq1	5'-TATGACAGGATAAATACACGCC-3'
	Forward	*1A8* Exon1	UGT1A8Ex1Fseq3	5'-ACTCAACCTCATACACTCTGGAG-3'
	Forward	*1A8* Exon1	UGT1A8Ex1Fseq2	5'-TGCTCCTCTTTCCTATGTCC-3'
	Reverse	*1A8* Exon1	UGT1A8Ex1Rseq1	5'-AACTTCGTACTTGTGCTTTCCA-3'
	Reverse	*1A8* Exon1	UGT1A8Ex1Rseq2	5'-ACTGGCAAAATAAATGTTCCTC-3'
	Reverse	*1A8* Exon1	UGT1A8Ex1Rseq3	5'-GCAACAAATGAAAATGTCAAATC-3'
	Forward	*1A9* 5'-Flank	UGT1A9pro-275Fseq	5'-GCTCTCGCAAGGATTGGG-3'
	Reverse	*1A9* 5'-Flank	UGT1A9pro-275Rseq	5'-CTTATGGTCTTTGCCTTGGG-3'
	Forward	*1A7* Exon1	UGT1A7F3-2	5'-TTTGAGGGCAGGTTCTATCTG-3'
	Reverse	*1A7* Exon1	UT1A71R3	5'-CAAAAACCATGAACTCCCGG-3'
	Forward	*1A7* Exon1	UT1A71F4	5'-TGGCAACTGGGAAGATCAC-3'
	Reverse	*1A7* Exon1	UT1A71R4	5'-GGACATAGGAAAGAGGAGCAG-3'
	Forward	*1A7* Exon1	UT1A71F5	5'-CTCCCTCCCCTCTGTGGTC-3'
	Reverse	*1A7* Exon1	UT1A71R5	5'-GCACTGGCTTTCCCTGATGAC-3'
	Forward	*1A7* Exon1	UGT1A7F6-2	5'-GAGGAACATTTATTTTGCCC-3'
	Reverse	*1A7* Exon1	UT1A71R6	5'-TACATATCAACAAGAGCTGC-3'
	Forward	*1A3* Exon1	UGT1A3seqF1	5'-GTGTTTTTCAAGATAGTC-3'
	Reverse	*1A3* Exon1	UGT1A3seqR1	5'-GCACATGGCGATCAAATTC-3'
	Forward	*1A3* Exon1	UGT1A3seqF2	5'-AGGCAGTGGTCCTCACCCCAGA-3'
	Reverse	*1A3* Exon1	UGT1A3seqR2	5'-AAGCATGGCAAATGTAGGACAGG-3'
	Forward	*1A3* Exon1	UGT1A3seqF3	5'-CCCTTCCTCCTATATTCCTAGA-3'
	Reverse	*1A3* Exon1	UGT1A3-1stR	5'-TTACAAACATTCGTGTCTACTT-3'

sequences). The PCR primers for the 2nd amplification of *1A10* and *1A9* were described previously.[37,38] Exon 1 in *1A3* and the promoter region of *1A9* were first directly amplified from genomic DNA (100 ng) using Ex-Taq as in the 2nd round of PCR described below. The second round of PCR consisted of one cycle at 94°C for 5 min, followed by 30 cycles of 94°C for 30 s, 55°C for 1 min, and 72°C for 2 min, and then a final extension for 7 min at 72°C. These PCR products were then treated with a PCR Product Pre-Sequencing Kit (USB Co., Cleveland, OH, USA) and directly sequenced on both strands using an ABI BigDye Terminator Cycle Sequencing Kit (Applied Biosystems, Foster City, CA, USA) and the primers listed in Table 2 (see 'Sequencing'). The excess dye was removed by a DyeEx96 kit (Qiagen, Hilden, Germany), and the eluates were analyzed on an ABI Prism 3700 DNA Analyzer (Applied Biosystems). All the SNPs were confirmed by repeating the PCR on genomic DNA and sequencing the newly generated PCR products.

Genotyping (pyrosequencing)

Genotyping was performed by pyrosequencing, except for *UGT1A4* 31C>T (R11W), 127delA (43fsX22: frameshift from codon 43 resulting in the termination at the 22nd codon, codon 65), 142T>G (L48V), 175delG (59fsX6), 271C>T (R91C), 325A>G (R109G), and IVS+1G>T, and *1A9* −126_−118 T9>T10 or T11, which were genotyped by direct sequencing because these polymorphisms were not clearly determined by pyrosequencing. Fragments were directly amplified from genomic DNA (10–15 ng) by Ex-Taq (1 U) with amplification primer pairs (either primer was biotinylated) (Table 3). The PCR conditions consisted of 1 cycle at 94°C for 5 min, followed by 50 cycles of 94°C for 30 s, 55°C for 30 s (except for *UGT1A* 1598A>C (H533P), in which annealing was carried out at 58°C for 45 s), and 72°C for 30 s. Primers for *1A1* −3279T>G, −40_−39 insTA, 211G>A (G71R), 247T>C (F83L), 686C>A (P229Q), and 1456T>G (Y486D) in common exon 5 were described

Table 3 Primers in pyrosequencing

	Gene	Detected variation	Amino-acid change	Primer name	Direction	Length	Sequences
Amplification	*UGT1A8*	518C>G	A173G	UGT1A8PyroF	Forward	387 bp	5′-bTACGAAGTTTGTTTTCTCTATTTCT-3′
				UGT1A8PyroR2b[a]	Reverse		5′-CTATTTCTAGGGCATTTTTGG-3′
	UGT1A10	4G>A, 177G>A, 200A>G	A2T, M59I, E67G	UGT1A10Pyro1F2-2	Forward	378 bp	5′-GGTCAGGTTTTGTGCCTGTAC-3′
				UGT1A10Pyro1R2b[a]	Reverse		5′-bATTGAGCATGGGCGAAAA-3′
	UGT1A10	605C>T	T202I	UGT1A10Pyro2F	Forward	123 bp	5′-CTTTCCTATGTCCCCAATGA-3′
				UGT1A10Pyro2Rb[a]	Reverse		5′-bGGCATTTCTAAAAAGATACTGG-3′
	UGT1A9	422C>G, 726T>G, 766G>A	S141C, Y242X, D256N	UGT1A9PyroF	Forward	589 bp	5′-TATTAATGGGTTCATACAATGACA-3′
				UGT1A9PyroRb[a]	Reverse		5′-bTTTTTTAATTTCCAAAGGTGAAG-3′
	UGT1A7	387T>G, 391C>A, 392G>A, 622T>C	N129K, R131K, W208R	UGT1A7PyroF	Forward	364 bp	5′-TATTAACAAGTTCATCCAATGGTA-3′
				UGT1A7PyroRb[a]	Reverse		5′-bTCTAAGACATTTTTGAAAAAATAGG-3′
	UGT1A6	19T>G, 269G>A, 308C>A	S7A, R90H, S103X	UGT1A6-1pyroF2	Forward	354 bp	5′-TTTAACTCTTTCCAGGATGGC-3′
				UGT1A6-1pyroR1b[a]	Reverse		5′-bCTGTACTCTGTCTGAGGAGCAGT-3′
	UGT1A6	541A>G, 552A>C	T181A, R184S	UGT1A6-2pyroF1b[a]	Forward	180 bp	5′-bACCATCTGTGTACCTCTTCAGG-3′
				UGT1A6-2pyroR1	Reverse		5′-AGACAATAAAATAGATAGGGCTCC-3′
	UGT1A3	17A>G, 31T>C	Q6R, W11R	UGT1A3pyroF1	Forward	379 bp	5′-CACTCTGTCTTCCAATTACACGT-3′
				UGT1A3pyroR3b[a]	Reverse		5′-bTCCACGAAATGGCATAGGT-3′
	UGT1A3	133C>T, 140T>C	R45W, V47A	UGT1A3pyroF1b[a]	Forward	379 bp	5′-bCACTCTGTCTTCCAATTACACGT-3′
				UGT1A3pyroR3	Reverse		5′-TCCACGAAATGGCATAGGT-3′
	UGT1A	1091C>T[b]	P364L[b]	UT1AP364L-F	Forward	226 bp	5′-TGAAACTCAGAGATGTAACTGCTG-3′
				UT1AP364L-Rb[a]	Reverse		5′-bCAGAAGTCATTTCCAGAACATTC-3′
	UGT1A	1598A>C[b]	H533P[b]	exonS-F	Forward	242 bp	5′-TGGGTGGAGTTTGTGATGA-3′
				bExonSR-H533P[a]	Reverse		5′-bCCTTATTTCCCACCCACTT-3′
	UGT1A 3′-UTR[c]	1813C>T[b], 1941C>G[b], 2042C>G[b]	*1B*[d]	UGT1AEx5-1BPyroFb[a]	Forward	332 bp	5′-bATTTGAATATGTATCGTGCCC-3′
				UGT1AEx5-1BPyroR	Reverse		5′-CATTCATTCATTTCACCTACACT-3′
Pyrosequencing	*UGT1A8*	518C>G	A173G	UGT1A8c518gPF			5′-CGCCAGGGGAATAG-3′
	UGT1A10	4G>A	A2T	UGT1A10g4aPF			5′-GGCTGCAGTTCTCTCA-3′
	UGT1A10	177G>A	M59I	UGT1A10g177aPF			5′-GCATGAGGTGGTTGTAG-3′
	UGT1A10	200A>G	E67G	UGT1A10a200gPF			5′-TGAGTTGGCAACTGG-3′
	UGT1A10	605C>T	T202I	UGT1A10c605tPF			5′-GGTTCTCAGATGCCATG-3′
	UGT1A9	422C>G	S141C	UGT1A9c422gPF			5′-AGAATACTTAAAGGAGAGT-3′
	UGT1A9	726T>G	Y242X	UGT1A9t726gPF			5′-AAACACCTGTTACGGAG-3′
	UGT1A9	766G>A	D256N	UGT1A9g766aPF			5′-GGTTGTTGCGAACG-3′
	UGT1A7	387T>G, 391C>A, 392G>A	N129K, R131K	UGT1A7387-392PF			5′-ATTGCAGGAGTTTGTTTA-3′
	UGT1A7	622T>C	W208R	UGT1A7c622tPF			5′-TTCAAGGAGAGAGTA-3′
	UGT1A6	19T>G	S7A	UGT1A6-1t19gPseq-F			5′-CCTGCCTCCTTCGC-3′
	UGT1A6	269G>A	R90H	UGT1A6-1g269aPseq-F			5′-AAGAAGAGCTGAAGAACC-3′
	UGT1A6	308C>A	S103X	UGT1A6-1c308aPseq-F			5′-AACAATCACTTTGCTGAG-3′
	UGT1A6	541A>G, 552A>C	T181A, R184S	UGT1A6-2a552cPseq-R			5′-GGACACAGGGTCTGG-3′
	UGT1A3	17A>G, 31T>C	Q6R, W11R	UGT1A3a17g-seqF			5′-TGGCCACAGGACTC-3′
	UGT1A3	133C>T, 140T>C	R45W, V47A	UGT1A3t140cPseq-R			5′-ATGGAGCTCCCGCAA-3′
	UGT1A	1091C>T[b]	P364L[b]	UGT1A1P364LPseqF			5′-TTTGCATCTCAGGTCAC-3′
	UGT1A	1598A>C[b]	H533P[b]	ExonS-1598F-Page			5′-CACAAATCCAAGACCC-3′
	UGT1A 3′-UTR[c]	1813C>T[b]	*1B*[d]	UGT1AEx5c1813tPseqR			5′-TCCTGATCAAAGACACC-3′
	UGT1A 3′-UTR[c]	1941C>G[b]	*1B*[d]	UGT1AEx5c1941gPseqR			5′-CAGTAGGGGCAGC-3′
	UGT1A 3′-UTR[c]	2042C>G[b]	*1B*[d]	UGT1AEx5c2042gPseqR			5′-TGGCACCTATGAAGCA-3′

[a]b: biotinylated.
[b]The positions of nucleotide and protein were numbered as those of *UGT1A1*.
[c]UTR: untranslated region.
[d]1813C>T, 1941C>G, and 2042C>G found in the 3′-UTR were named haplotype *1B*.[19]

previously.[39] Biotinylated single-stranded DNA fragments were generated as described previously.[39] Briefly, PCR products were mixed with streptavidin beads for 10 min. The beads were transferred to a MultiScreen-HV Plate (Millipore Corporation, Billerica, MA, USA), and the buffer was removed by vacuum. DNA attached to the beads was denatured, washed twice, and then suspended in 20 mM Tris-acetate containing 2 mM Mg-acetate (pH 7.6). After transferring to a 96-well PSQ plate (Pyrosequencing AB, Uppsala, Sweden), 10 pmol of the sequencing primer (PAGE-purified grade) (Table 3) for SNP analysis was added to the single-stranded fragments. The mixture was incubated at 95°C for 2 min, and then cooled to room temperature for annealing. An automated pyrosequencing instrument, the PSQ™96MA (Pyrosequencing AB), and the PSQ 96 SNP reagent kit (Pyrosequencing AB) were used to perform the genotyping. To validate the typing methods, the results for 48 samples were confirmed to be identical to those obtained by direct sequencing (data not shown).

LD and haplotype analysis

Hardy–Weinberg equilibrium analysis and LD analysis were performed using SNPAlyze software (version 3.2). (Dynacom Co. Ltd., Yokohama, Japan), and pairwise two-dimensional maps between SNPs were obtained for the $|D'|$, χ^2, and r^2 values. Some of the haplotypes were unambiguously determined from the subjects with homozygous SNPs at all sites or a heterozygous SNP at only one site. Separately, the diplotype configurations (combination of haplotypes) were inferred by an expectation-maximization-based program, LDSUPPORT, which determines the posterior probability distribution of the diplotype configuration for each subject based on the estimated haplotype frequencies.[40]

The diplotype configurations of the subjects were inferred with probability (certainty) values over 0.96 for 184, 191, and 188 out of 196 subjects in the *UGT1A8-1A10* block (*Block 8/10*), the *1A9-1A7-1A6* block (*Block 9/6*), and the *1A3-1A1* block (*Block 3/1*), respectively. The *Block 4* (*1A4*) haplotypes were described previously.[21] Note that the predictability for the extremely rare haplotypes inferred from only one subject is known to be low in some cases. Haplotype analysis was also performed among the representative SNPs in *Block 9/6*, *Block 4*, and *Block 3/1* by LDSUPPORT software.

Abbreviations

LD	*linkage disequilibrium*
PCR	*polymerase chain reaction*
SN-38	*7-ethyl-10-hydroxycamptothecin*
SNP	*single nucleotide polymorphism*
UGT	*UDP-glucuronosyltransferase*
UTR	*untranslated region*

Acknowledgments

This study was supported in part by the Program for Promotion of Fundamental Studies in Health Sciences and by the Health and Labour Sciences Research Grants from Ministry of Health, Labour and Welfare, and the grant from the Japan Health Sciences Foundation. We thank Ms Chie Sudo for her secretarial assistance.

DUALITY OF INTEREST

None declared.

References

1 Radominska-Pandya A, Czernik PJ, Little JM. Structural and functional studies of UDP-glucuronosyltransferases. *Drug Metab Rev* 1999; 31: 817–899.
2 Tukey RH, Strassburg CP. Genetic multiplicity of the human UDP-glucuronosyltransferases and regulation in the gastrointestinal tract. *Mol Pharmacol* 2001; 59: 405–414.
3 Gong QH, Cho JW, Huang T, Potter C, Gholami N, Basu NK *et al.* Thirteen UDPglucuronosyltransferase genes are encoded at the human UGT1 gene complex locus. *Pharmacogenetics* 2001; 11: 357–368.
4 Metz RP, Ritter JK. Transcriptional activation of the UDP-glucuronosyltransferase 1A7 gene in rat liver by aryl hydrocarbon receptor ligands and oltipraz. *J Biol Chem* 1998; 273: 5607–5614.
5 Guillemette C. Pharmacogenomics of human UDP-glucuronosyltransferase enzymes. *Pharmacogenomics J* 2003; 3: 136–158.
6 Guillemette C, Ritter JK, Auyeung DJ, Kessler FK, Housman DE. Structural heterogeneity at the UDP-glucuronosyltransferase 1 locus: functional consequences of three novel missense mutations in the human UGT1A7 gene. *Pharmacogenetics* 2000; 10: 629–644.
7 Gagne JF, Montminy V, Belanger P, Journault K, Gaucher G, Guillemette C. Common human UGT1A polymorphisms and the altered metabolism of irinotecan active metabolite 7-ethyl-10-hydroxycamptothecin (SN-38). *Mol Pharmacol* 2002; 62: 608–617.
8 Huang YH, Galijatovic A, Nguyen N, Geske D, Beaton D, Green J *et al.* Identification and functional characterization of UDP-glucuronosyltransferases UGT1A8*1, UGT1A8*2 and UGT1A8*3. *Pharmacogenetics* 2002; 12: 287–297.
9 Elahi A, Bendaly J, Zheng Z, Muscat JE, Richie Jr JP, Schantz SP *et al.* Detection of UGT1A10 polymorphisms and their association with orolaryngeal carcinoma risk. *Cancer* 2003; 98: 872–880.
10 Jinno H, Saeki M, Saito Y, Tanaka-Kagawa T, Hanioka N, Sai K *et al.* Functional characterization of human UDP-glucuronosyltransferase 1A9 variant, D256N, found in Japanese cancer patients. *J Pharmacol Exp Ther* 2003; 306: 688–693.
11 Jinno H, Saeki M, Tanaka-Kagawa T, Hanioka N, Saito Y, Ozawa S *et al.* Functional characterization of wild-type and variant (T202I and M59I) human UDP-glucuronosyltransferase 1A10. *Drug Metab Dispos* 2003; 31: 528–532.
12 Villeneuve L, Girard H, Fortier LC, Gagne JF, Guillemette C. Novel functional polymorphisms in the UGT1A7 and UGT1A9 glucuronidating enzymes in Caucasian and African-American subjects and their impact on the metabolism of 7-ethyl-10-hydroxycamptothecin and flavopiridol anticancer drugs. *J Pharmacol Exp Ther* 2003; 307: 117–128.
13 Ehmer U, Vogel A, Schutte JK, Krone B, Manns MP, Strassburg CP. Variation of hepatic glucuronidation: novel functional polymorphisms of the UDP-glucuronosyltransferase UGT1A4. *Hepatology* 2004; 39: 970–977.
14 Nagar S, Zalatoris JJ, Blanchard RL. Human UGT1A6 pharmacogenetics: identification of a novel SNP, characterization of allele frequencies and functional analysis of recombinant allozymes in human liver tissue and in cultured cells. *Pharmacogenetics* 2004; 14: 487–499.
15 Jinno H, Tanaka-Kagawa T, Hanioka N, Saeki M, Ishida S, Nishimura T *et al.* Glucuronidation of 7-ethyl-10-hydroxycamptothecin (SN-38), an active metabolite of irinotecan (CPT-11), by human UGT1A1 variants, G71R, P229Q, and Y486D. *Drug Metab Dispos* 2003; 31: 108–113.
16 Judson R, Stephens JC, Windemuth A. The predictive power of haplotypes in clinical response. *Pharmacogenomics* 2000; 1: 15–26.
17 Kohle C, Mohrle B, Munzel PA, Schwab M, Wernet D, Badary OA *et al.* Frequent co-occurrence of the TATA box mutation associated with Gilbert's syndrome (UGT1A1*28) with other polymorphisms of the

UDP-glucuronosyltransferase-1 locus (UGT1A6*2 and UGT1A7*3) in Caucasians and Egyptians. *Biochem Pharmacol* 2003; **65**: 1521–1527.
18 Carlini LE, Meropol NJ, Bever J, Andria ML, Hill T, Gold P *et al.* UGT1A7 and UGT1A9 polymorphisms predict response and toxicity in colorectal cancer patients treated with capecitabine/irinotecan. *Clin Cancer Res* 2005; **11**: 1226–1236.
19 Sai K, Saeki M, Saito Y, Ozawa S, Katori N, Jinno H *et al.* UGT1A1 Haplotypes associated with reduced glucuronidation and increased serum bilirubin in irinotecan-administered Japanese cancer patients. *Clin Pharmacol Ther* 2004; **75**: 501–515.
20 Saeki M, Saito Y, Jinno H, Sai K, Kaniwa N, Ozawa S *et al.* Genetic polymorphisms of *UGT1A6* in a Japanese population. *Drug Metab Pharmacokinet* 2005; **20**: 85–90.
21 Saeki M, Saito Y, Jinno H, Sai K, Hachisuka A, Kaniwa N *et al.* Genetic variations and haplotypes of *UGT1A4* in a Japanese population. *Drug Metab Pharmacokinet* 2005; **20**: 144–151.
22 Iwai M, Maruo Y, Ito M, Yamamoto K, Sato H, Takeuchi Y. Six novel UDP-glucuronosyltransferase (UGT1A3) polymorphisms with varying activity. *J Hum Genet* 2004; **49**: 123–128.
23 Kozak M. Recognition of AUG and alternative initiator codons is augmented by G in position +4 but is not generally affected by the nucleotides in positions +5 and +6. *EMBO J* 1997; **16**: 2482–2492.
24 Yamanaka H, Nakajima M, Katoh M, Hara Y, Tachibana O, Yamashita J *et al.* A novel polymorphism in the promoter region of human UGT1A9 gene (UGT1A9*22) and its effects on the transcriptional activity. *Pharmacogenetics* 2004; **14**: 329–332.
25 Lankisch TO, Vogel A, Eilermann S, Fiebeler A, Krone B, Barut A *et al.* Identification and characterization of a functional TATA box polymorphism of the UDP glucuronosyltransferase 1A7 gene. *Mol Pharmacol* 2005; **67**: 1732–1739.
26 Ando M, Ando Y, Sekido Y, Ando M, Shimokata K, Hasegawa Y. Genetic polymorphisms of the UDP-glucuronosyltransferase 1A7 gene and irinotecan toxicity in Japanese cancer patients. *Jpn J Cancer Res* 2002; **93**: 591–597.
27 Huang MJ, Yang SS, Lin MS, Huang CS. Polymorphisms of uridine-diphosphoglucuronosyltransferase 1A7 gene in Taiwan Chinese. *World J Gastroenterol* 2005; **11**: 797–802.
28 Innocenti F, Liu W, Chen P, Desai AA, Das S, Ratain MJ. Haplotypes of variants in the UDP-glucuronosyltransferase1A9 and 1A1 genes. *Pharmacogenet Genomics* 2005; **15**: 295–301.
29 Ciotti M, Basu N, Brangi M, Owens IS. Glucuronidation of 7-ethyl-10-hydroxycamptothecin (SN-38) by the human UDP-glucuronosyltransferases encoded at the UGT1 locus. *Biochem Biophys Res Commun* 1999; **260**: 199–202.
30 Lepine J, Bernard O, Plante M, Tetu B, Pelletier G, Labrie F *et al.* Specificity and regioselectivity of the conjugation of estradiol, estrone, and their catecholestrogen and methoxyestrogen metabolites by human uridine diphospho-glucuronosyltransferases expressed in endometrium. *J Clin Endocrinol Metab* 2004; **89**: 5222–5232.
31 Basu NK, Kubota S, Meselhy MR, Ciotti M, Chowdhury B, Hartori M *et al.* Gastrointestinally distributed UDP-glucuronosyltransferase 1A10, which metabolizes estrogens and nonsteroidal anti-inflammatory drugs, depends upon phosphorylation. *J Biol Chem* 2004; **279**: 28320–28329.
32 Turgeon D, Chouinard S, Belanger P, Picard S, Labbe JF, Borgeat P *et al.* Glucuronidation of arachidonic and linoleic acid metabolites by human UDP-glucuronosyltransferases. *J Lipid Res* 2003; **44**: 1182–1191.
33 Little JM, Kurkela M, Sonka J, Jantti S, Ketola R, Bratton S *et al.* Glucuronidation of oxidized fatty acids and prostaglandins B1 and E2 by human hepatic and recombinant UDP-glucuronosyltransferases. *J Lipid Res* 2004; **45**: 1694–1703.
34 Beutler E, Gelbart T, Demina A. Racial variability in the UDP-glucuronosyltransferase 1 (UGT1A1) promoter: a balanced polymorphism for regulation of bilirubin metabolism? *Proc Natl Acad Sci USA* 1998; **95**: 8170–8174.
35 Sugatani J, Yamakawa K, Yoshinari K, Machida T, Takagi H, Mori M *et al.* Identification of a defect in the UGT1A1 gene promoter and its association with hyperbilirubinemia. *Biochem Biophys Res Commun* 2002; **292**: 492–497.
36 Oguri T, Takahashi T, Miyazaki M, Isobe T, Kohno N, Mackenzie PI *et al.* UGT1A10 is responsible for SN-38 glucuronidation and its expression in human lung cancers. *Anticancer Res* 2004; **24**: 2893–2896.
37 Saeki M, Ozawa S, Saito Y, Jinno H, Hamaguchi T, Nokihara H *et al.* Three novel single nucleotide polymorphisms in UGT1A10. *Drug Metab Pharmacokinet* 2002; **17**: 488–490.
38 Saeki M, Saito Y, Jinno H, Sai K, Komamura K, Ueno K *et al.* Three novel single nucleotide polymorphisms in UGT1A9. *Drug Metab Pharmacokinet* 2003; **18**: 146–149.
39 Saeki M, Saito Y, Jinno H, Tohkin M, Kurose K, Kaniwa N *et al.* Comprehensive UGT1A1 genotyping in a Japanese population by pyrosequencing. *Clin Chem* 2003; **49**: 1182–1185.
40 Kitamura Y, Moriguchi M, Kaneko H, Morisaki H, Morisaki T, Toyama K *et al.* Determination of probability distribution of diplotype configuration (diplotype distribution) for each subject from genotypic data using the EM algorithm. *Ann Hum Genet* 2002; **66**: 183–193.

Strahlentherapie
und Onkologie

Original Article

High-Dose-Rate Brachytherapy for Small-Sized Peripherally Located Lung Cancer

Fumio Imamura[1], Kiyonobu Ueno[1], Yoko Kusunoki[2], Junji Uchida[1], Mana Yoshimura[1], Masahiko Koizumi[3], Hideya Yamasaki[3], Kinji Nishiyama[3]

Background: The demand for minimally invasive therapies is increasing in the treatment of small peripheral non-small cell lung cancer (NSCLC).
Patients and Methods: Twelve patients with T1–2 N0 M0 peripheral NSCLC were treated by high-dose-rate brachytherapy with ^{192}Ir radioactive source.
Results: A ^{192}Ir source was introduced into the tumors percutaneously in five patients (percutaneous brachytherapy) or transbronchially in seven patients (transbronchial brachytherapy). Whereas irradiation was performed with a single fraction of 20 Gy in percutaneous brachytherapy, it was hypofractionated from 5 × 5 Gy to 2 × 12.5 Gy in transbronchial brachytherapy. Complications were generally mild in all patients, although focal radiation pneumonitis was observed in most patients. Primary recurrence occurred in three patients, including one with a T2 tumor and one treated by brachytherapy as a salvage treatment for recurrence after conformal radiotherapy. When brachytherapy is evaluated as a primary treatment for T1 N0 M0 NSCLC, local control rate is 88.9% and estimated 5-year survival rate is between 60% and 70%.
Conclusion: Brachytherapy has a potential to be a method to treat peripheral T1 N0 M0 NSCLC.

Key Words: Lung cancer · Brachytherapy · T1 N0 M0 · Peripheral · Transbronchial · Percutaneous

Strahlenther Onkol 2006;182:703–7
DOI 10.1007/s00066-006-1536-6

High-Dose-Rate-Brachytherapie bei kleinem peripheren Bronchialkarzinom

Hintergrund: Das Erfordernis minimalinvasiver Eingriffe in der Behandlung kleiner, peripherer, nichtkleinzelliger Bronchialkarzinome (NSCLC) nimmt zu.
Patienten und Methodik: Zwölf Patienten mit peripherem NSCLC der Stadien T1–2 N0 M0 erhielten eine High-Dose-Rate-Brachytherapie mit radioaktiver ^{192}Ir-Quelle.
Ergebnisse: Die ^{192}Ir-Quelle wurde bei fünf Patienten über einen perkutanen Zugang (perkutane Brachytherapie) und bei sieben Patienten über einen bronchialen Zugang (transbronchiale Brachytherapie) eingeführt. Bei der perkutanen Brachytherapie wurde die Bestrahlung mit einer Einzeitdosis von 20 Gy durchgeführt, bei der transbronchialen Brachytherapie hypofraktioniert mit 5 × 5 Gy bis 2 × 12,5 Gy. Komplikationen waren im Allgemeinen geringgradig ausgeprägt, allerdings wurde bei den meisten Patienten eine fokale Strahlenpneumopathie beobachtet. Bei drei Patienten trat ein Lokalrezidiv auf (zwei Patienten mit T2-Tumor und ein Patient mit Brachytherapie als Salvage-Behandlung wegen eines Rezidivs nach konventioneller Strahlentherapie). Für die Brachytherapie in der Primärbehandlung von NSCLC des Stadiums T1 N0 M0 beträgt die lokale Kontrollrate 88,9%, und die geschätzte 5-Jahre-Überlebensrate liegt bei 60–70%.
Schlussfolgerung: Die Brachytherapie ist eine effektive Behandlungsmethode bei peripherem NSCLC des Stadiums T1 N0 M0.

Schlüsselwörter: Bronchialkarzinom · Brachytherapie · T1 N0 M0 · Peripher · Transbronchial · Perkutan

[1] Department of Pulmonary Oncology, Osaka Medical Center for Cancer and Cardiovascular Diseases, Osaka, Japan,
[2] Department of Field Work and Epidemiology, Osaka Medical Center for Cancer and Cardiovascular Diseases, Osaka, Japan,
[3] Department of Radiation Therapy, Osaka Medical Center for Cancer and Cardiovascular Diseases, Osaka, Japan.

Received: October 19, 2005; accepted: August 18, 2006

Introduction

Although surgical resection is a standard treatment for stage I non-small cell lung cancer (NSCLC), the aging of population requires minimally invasive therapies in its treatment. Conventional external radiation of 55–75 Gy is an alternative in this setting, but it associates with an unacceptably low 5-year survival rate, around 20% [1–3, 6, 10].

Brachytherapy is a radiation therapy using a small radioactive source to treat various cancers, and has the potential advantage of providing the tumor-bearing area with a higher radiation dose relative to doses received by the surrounding normal tissues. We have already reported a patient with peripheral T1 N0 M0 pulmonary adenocarcinoma who was successfully treated by CT-guided single-fraction interstitial brachytherapy alone [5]. After confirming the safety and efficacy of brachytherapy in the peripheral lung through the observation of this patient over 5 years, we have built on our experiences of brachytherapy for peripheral NSCLC.

Patient and Methods

From April 1996, twelve patients with peripheral T1–2 N0 M0 NSCLC received CT-guided brachytherapy (Table 1). A transbronchial approach was applied to eight patients, but failed in one patient because of poor access to the tumor. Five patients including this patient were treated by the percutaneous method. The patients were relatively high-aged (53–85 years old), and mostly medically inoperable due to concomitant medical illnesses or refusal of surgical treatment. Respiratory function of the patients was generally poor.

A ^{192}Ir source was tentatively introduced into the lesions either percutaneously (percutaneous brachytherapy) or transbronchially (transbronchial brachytherapy; Figure 1). In percutaneous brachytherapy, tumors were punctured percutaneously with a 21-G needle under fluorography and CT guidance in local anesthesia, and an applicator tube with an open edge was connected to the needle. In transbronchial brachytherapy, an applicator tube with a blind edge was directly introduced into the tumor via bronchoscope under fluorography and CT guidance (Figure 2).

Target volumes and reference points were defined by CT examination before each treatment. Gross tumor volume (GTV) was defined as the mass shadow depicted on CT images in lung window. Clinical target volume (CTV) was equal to GTV without including regional lymph nodes, and margins of 1 cm were added to contour planning target volume (PTV). In transbronchial brachytherapy, a dummy wire was inserted into the applicator before treatment, and the reference point was determined as the furthest point in the tumor from the dummy wire. The dwell positions were determined on chest X-ray and CT images to treat PTV adequately; the dwell time was calculated to deliver the prescribed dose to the reference point without optimization. Thereafter, the real source was pushed into the applicator by step-backward design with step sizes of the source length. In percutaneous brachytherapy, the reference point was determined as the furthest point in the tumor from the needle. Planning and treatment were performed similarly.

The dose distribution was calculated by Cadplan BT (version 1.1.15) till 2003 and later by BrachyVision (version 6.1.13). Brachytherapy was performed using a ^{192}Ir radioactive source, which was equipped with a wire of 0.635 mm diameter connected to a computer-driven remote afterloader (Varisource, Varian Medical System). The diameter and length of a ^{192}Ir source were 0.52 mm and 10 mm, respectively, in the beginning, but later a ^{192}Ir source of 5 mm length became available. In transbrochial brachytherapy, irradiation by five fractions of 5 Gy (total 25 Gy) was first adopted, then was hypofractionated, and currently, irradiation by two fractions of 12.5 Gy (total 25 Gy) is being done. In percutaneous brachytherapy, single 20-Gy fraction irradiation was performed. To avoid pneumothorax, transbronchial brachytherapy was generally selected as the first-choice treatment.

Table 1. Patient characteristics. BI: Brickman index; SCLC: small cell lung carcinoma.

Tabelle 1. Patientencharakteristika. BI: Brickman-Index; SCLC: kleinzelliges Bronchialkarzinom.

	Patients (n)
Mean age	74.5 years (53–85 years)
Male/female	10/2
Stage	
• T1 N0 M0	11
• T2 N0 M0	1
Number of cancers (synchronous)	
• Single	6
• Double	4 (3)
• Quartet	2 (1)
Histology	
• Adenocarcinoma	5
• Squamous cell carcinoma	6
• SCLC	1
Tumor size, mean 25.4 mm	
• ≤ 20 mm	5
• 21–30 mm	6
• ≥ 31 mm	1
Smoking (BI)	400–2,400 (median 1,200)
Primary reason for selecting this treatment	
• Impaired cardiopulmonary function	6
• Inoperable	3
• Refusal of surgery	2
• Recurrence of tumor	1
Introduction of radioactive source	
• Percutaneous	5
• Transbronchial	8 (including 1 failure[a])
Pretreatment to the lesion	
• None	11
• Conformal irradiation	1

[a] successfully treated by percutaneous brachytherapy

However, since the percutaneous approach is easier to access lesions than the transbronchial one, percutaneous brachytherapy was done for the patients who had negligible risk of pneumothorax or were acceptable for pneumothorax.

Complete (CR) and partial regression (PR) of the tumor were defined as reduction by 100% and > 50% of maximal tumor area lasting for at least 1 month, respectively; progressive disease (PD) was defined as increment by > 25% of maximal tumor area. Stable disease (SD) was defined as the change that met neither CR, PR, nor PD. The evaluation of response was planned at 1, 3, 6, and 12 months following treatment, and every 6 months thereafter.

Results

Although moderate radiation pneumonitis appeared in one patient who had undergone conformal radiotherapy for the same tumor previously and mild pneumothorax was observed in one patient who received percutaneous brachytherapy, brachytherapy was safe and radiation pneumonitis was generally mild. We have already reported that our first percutaneous single-fraction brachytherapy for peripheral T1N0M0 NSCLC resulted in no appreciable short-term complications [5]. Follow-up of this case showed that the tumor and surrounding normal lung irradiated formed a nodule that remained similar-sized for approximately 7.5 years (Figure 3). The lung parenchyma surrounding the nodule seems to shrink, but no appreciable radiation pneumonitis has been observed during the entire observation period. The nodule is possibly focal radiation fibrosis, although pathologic examination was not performed.

The therapeutic parameters were shown in Table 2. The radiation time period was 518 ± 399 s, ranging between 123 and 1,559 s, depending on several factors including tumor size, location of an applicator in the tumor, and activity of radioactive source. V_{100} had a tendency to be smaller in percutaneous (20 ± 15 ml) than in transbronchial (49 ± 37 ml) brachytherapy.

Three (25%), four (33.3%), and five patients (41.7%) showed CR, PR, and SD, respectively, resulting in a response rate of 58.3%. So far, three patients have experienced dis-

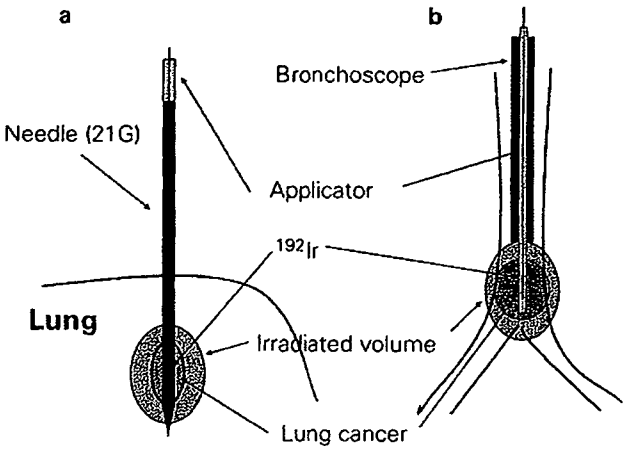

Figures 1a and 1b. Schema of percutaneous and transbronchial brachytherapy. The radioactive iridium source is introduced via needle into the tumor (a), or it reaches the tumor through an applicator tube via bronchoscope (b).

Abbildungen 1a und 1b. Schematische Darstellung der perkutanen und der transbronchialen Brachytherapie. Die radioaktive Iridium-Quelle wird mit Hilfe einer Nadel in den Tumor eingeführt (a) oder erreicht ihn über einen bronchoskopisch eingeführten Applikator (b).

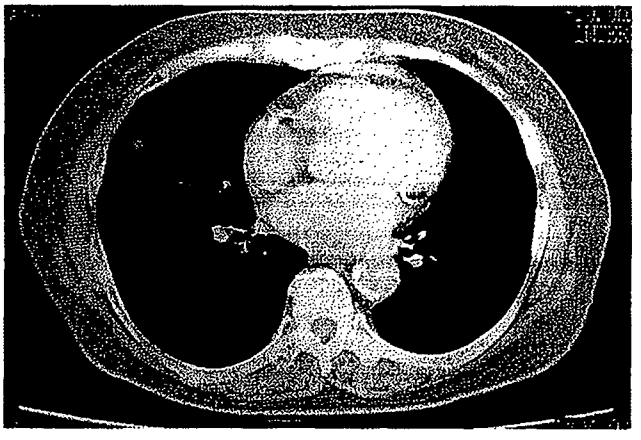

Figure 2a – Abbildung 2a

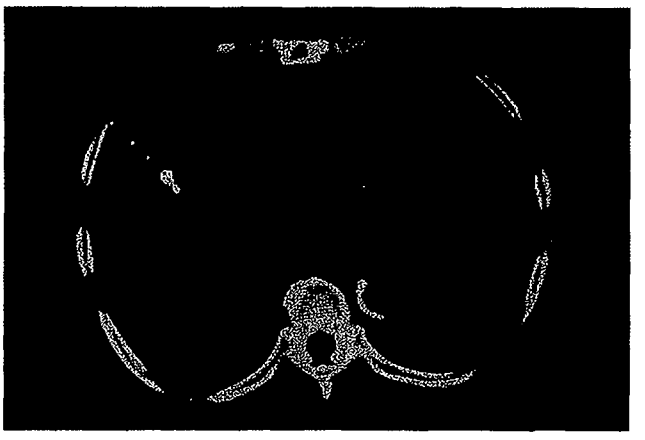

Figure 2b – Abbildung 2b

Figures 2a and 2b. Transbronchial brachytherapy. T1N0M0 pulmonary adenocarcinoma is present in right S4 (a). An applicator tube is introduced into the tumor via bronchoscope (b).

Abbildungen 2a und 2b. Transbronchiale Brachytherapie. Es liegt ein T1N0M0-Adenokarzinom der Lunge rechts in S4 vor (a). Der Applikator wird bronchoskopisch in den Tumor gebracht (b).

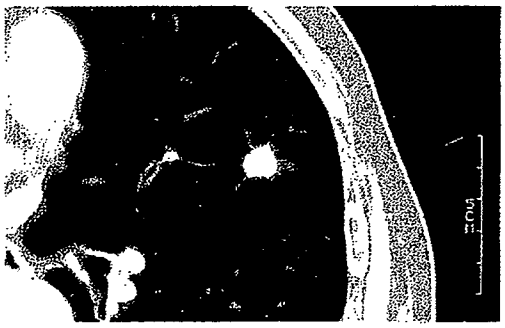

Figure 3a – Abbildung 3a

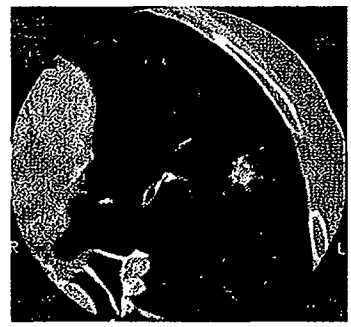

Figure 3b – Abbildung 3b

Figure 3c – Abbildung 3c

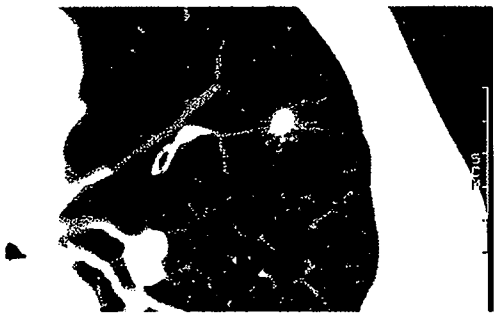

Figure 3d – Abbildung 3d

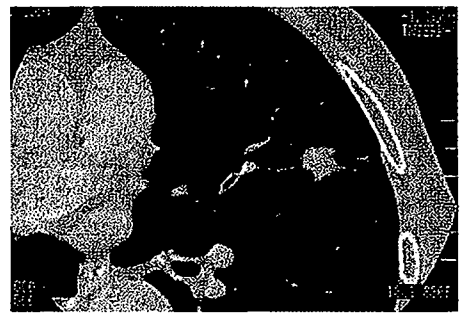

Figure 3e – Abbildung 3e

Figures 3a to 3e. Clinical course of the lesion treated by percutaneous brachytherapy. A nodule in the left middle lobe was irradiated by brachytherapy (a). 3 months (b) and 9 months (c) after the treatment, the nodule stayed in similar size, whereas the surrounding pulmonary parenchyma showed a tendency to shrink. During 7.5-year observation (d, e), the nodule has remained almost stable in size.

Abbildungen 3a bis 3e. Klinischer Verlauf nach perkutaner Brachytherapie eines Karzinoms. Ein Knoten im linken Mittellappen wurde brachytherapeutisch bestrahlt (a). Drei (b) und neun (c) Monate nach der Behandlung war die Größe des Knotens kaum verändert, während das umgebende Lungenparenchym eine Tendenz zum Schrumpfen zeigte. Während der Nachbeobachtungszeit von 7,5 Jahren (d, e) blieb die Größe des Karzinoms fast stabil.

ease recurrence, which occurred at 32 months, 12 months, and 13 months after the treatment, respectively. When brachytherapy was evaluated as an initial treatment for T1N0M0 NSCLC, local relapse occurred in one patient. Projected 5-year survival rate of all cases is about 50% and that of the patients in T1N0M0 between 60% and 70% (Figure 4).

Table 2. Parameters in brachytherapy. SD: standard deviation; V_{100}: volume irradiated at the dose over that at the reference point.

Tabelle 2. Parameter der Brachytherapie. SD: Standardabweichung; V_{100}: Volumen, das mit einer höheren als der Referenzpunkt-Dosis bestrahlt wird.

Fractionation		
Transbronchial		
• 5 Gy × 5 fractions	1	
• 4 Gy × 2 fractions + 5 Gy × 2 fractions	1	
• 7 Gy × 3 fractions	3	
• 12.5 Gy × 2 fractions	2	
Percutaneous		
• 20 Gy × 1 fraction	5	
Irradiation time per fraction	**Mean ± SD**	**Range**
Transbronchial	500 ± 491 s	
Percutaneous	542 ± 276 s	
Overall	518 ± 399 s	123–1,559 s
V_{100}*	**Mean ± SD**	**Range**
Transbronchial	49 ± 37 ml	
Percutaneous	20 ± 15 ml	
Overall	37 ± 33 ml	5–102 ml

*mean ± SD in each approach

Discussion

This study showed that brachytherapy was safe and effective in the treatment of peripheral small NSCLC. One patient experienced minimal pneumothorax due to percutaneous puncture, but no treatment was necessary. Radiation pneumonitis was mild and focal, reflecting limited distribution of radiation dose in brachytherapy. Whereas brachytherapy for central airway tumors is reported to sometimes induce necrotizing bronchitis and severe hemoptysis, no hemoptysis was observed in our study. Percutaneous brachytherapy has an advantage in that a ^{192}Ir needle can be introduced almost in the center of tumors. In transbronchial brachytherapy, a ^{192}Ir needle is in the bronchial tree, and therefore, it is difficult to put the radioactive source in the center of tumor.

Primary recurrence was observed in three patients. In one of them, brachytherapy was performed as a salvage treatment for recurrence after conformal radiotherapy and in an-

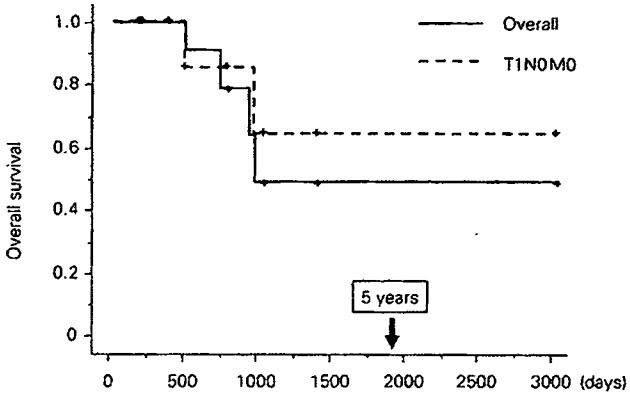

Figure 4. Kaplan-Meier analysis of overall survival of the patients treated by brachytherapy alone. A dotted line is a survival curve of the patients with T1N0M0 lung cancer. Projected 5-year survival rates are around 50% in all patients and between 60% and 70% in the patients with T1N0M0 tumor, respectively.

Abbildung 4. Kaplan-Meier-Analyse des Gesamtüberlebens der ausschließlich brachytherapeutisch versorgten Patienten. Die gestrichelte Linie ist die Überlebenskurve der Patienten mit T1N0M0-Lungenkrebs. Die prospektiven 5-Jahres-Überlebensraten liegen für alle Patienten bei rund 50%, und zwischen 60% und 70% bei Patienten mit T1N0M0-Karzinom.

other with T2 tumor. In the latter systemic recurrence was also observed. The local control rate for primary T1N0M0 NSCLC by brachytherapy is 90% (9/10), and no systemic recurrence has occurred.

Recently, stereotactic (SRT) or conformal radiotherapy (CRT) is widely used for inoperable T1N0M0 NSCLC, and radiofrequency ablation is also applied. The comparison of brachytherapy with these methods is necessary. Although brachytherapy for centrally located NSCLC is studied extensively [7], reports on its application to peripheral NSCLC are still limited [4, 9, 12, 14]. Recently, image-guided brachytherapy is being developed for the tumors in several organs [4, 8, 11, 13]. Considering the multifocal nature of NSCLC sometimes seen in certain patients, overlap of radiation beams will become a serious problem in CRT and SRT. Because of the steep gradient of radiation doses, brachytherapy is especially useful in the treatment of patients with poor respiratory reserve or multiple early lung cancer.

References

1. Catalano G, Jereczek-Fossa BA, De Pas T, et al. Three-times-daily radiotherapy with induction chemotherapy in locally advanced non-small cell lung cancer. Feasibility and toxicity study. Strahlenther Onkol 2005;181:363–71.
2. Gagel B, Piroth M, Pinkawa M, et al. Gemcitabine concurrent with thoracic radiotherapy after induction chemotherapy with gemcitabine/vinorelbine in locally advanced non-small cell lung cancer. A phase I study. Strahlenther Onkol 2006;182:263–9.
3. Haffty BG, Goldberg NB, Gerstley J, et al. Results of radical radiation therapy in clinical stage I, technically operable non-small cell lung cancer. Int J Radiat Oncol Biol Phys 1988;15:69–73.
4. Harms W, Krempien R, Grehn C, et al. Electromagnetically navigated brachytherapy as a new treatment option for peripheral pulmonary tumors. Strahlenther Onkol 2006;182:108–11.
5. Imamura F, Chatani M, Nakayama T, et al. Percutaneous brachytherapy for small-sized non-small cell lung cancer. Lung Cancer 1999;24:169–74.
6. Jeremic B, Shibamoto Y, Acimovic L, et al. Hyperfractionated radiotherapy alone for clinical stage I non-small cell lung cancer. Int J Radiat Oncol Biol Phys 1977;38:521–5.
7. Macha HN, Freitag L. The role of brachytherapy in the treatment and control of central bronchial carcinoma. Monaldi Arch Chest Dis 1996;51:325–8.
8. Martin T, Baltas D, Kurek R, et al. 3-D conformal HDR brachytherapy as monotherapy for localized prostate cancer. A pilot study. Strahlenther Onkol 2004;180:225–32.
9. Martinez-Monge R, Garran C, Vivas I, et al. Percutaneous CT-guided ^{103}Pd implantation for the medically inoperable patient with T1N0M0 non-small cell lung cancer: a case report. Brachytherapy 2004;3:179–81.
10. Morita K, Fuwa N, Suzuki Y, et al. Radical radiotherapy for medically inoperable non-small cell lung cancer in clinical stage I: a retrospective analysis of 149 patients. Radiother Oncol 1997;42:31–6.
11. Niehoff P, Dietrich J, Ostertag H, et al. High-dose-rate (HDR) or pulsed-dose-rate (PDR) perioperative interstitial intensity-modulated brachytherapy (IMBT) for local recurrences of previously irradiated breast or thoracic wall following breast cancer. Strahlenther Onkol 2006;182:102–7.
12. Raben A, Mychalczak B. Brachytherapy for non-small cell lung cancer and selected neoplasms of the chest. Chest 1997;112(Suppl 4):276S–86S.
13. Ricke J, Wust P, Stohlmann A, et al. CT-guided brachytherapy. A novel percutaneous technique for interstitial ablation of liver metastases. Strahlenther Onkol 2004;180:274–80.
14. Ricke J, Wust P, Wieners G, et al. CT-guided interstitial single-fraction brachytherapy of lung tumors: phase I results of a novel technique. Chest 2005;127:2237–42.

Address for Correspondence
Fumio Imamura
Department of Pulmonary Oncology
Osaka Medical Center for Cancer and Cardiovascular Diseases
1-3-3 Nakamichi Higashinari-ku
Osaka 537-8511
Japan
Phone (+81/6) 6972-1181, Fax -6971-7636
e-mail: imamura-fu@mc.pref.osaka.jp

特集　非小細胞肺がんに対する化学療法の最新動向

III期非小細胞肺がんの放射線化学療法*

原田英博**
新明裕子**
大江裕一郎**

Key Words : chemoradiotherapy, non-small cell lung cancer, fractionation, target-based drug

はじめに

わが国では肺がん死亡者数は年々増加傾向にあり，2004年には約6万人の患者が肺がんで死亡している．今後も肺がんの罹患率は上昇することが予測されており，とくに人口の高齢化に伴った高齢者の肺がん患者の増加は著しい．肺がんの約80%を占める非小細胞肺がんのうち早期症例に対する手術は根治を目標とする治療法として効果的ではあるが，切除対象になる症例はわずかに30%程度にしかすぎない．切除不能の非小細胞肺がんのうち遠隔転移や悪性胸水を有さない局所進行非小細胞肺がんに対しては，局所効果を高め，潜在的遠隔転移を抑制させる目的から放射線治療と化学療法を同時併用する治療法が標準的治療と考えられている．非小細胞肺がんの治療として，プラチナ製剤といわゆる第3世代抗がん剤を2剤併用する化学療法は，生存率改善，転移抑制，症状緩和に寄与するこ

表1　切除不能局所進行非小細胞肺がんに対する放射線化学療法とpN2非小細胞肺がんに対する外科切除の成績

試験		JCOG 9202	JCOG 9209
対象		切除不能例	切除可能，pN2
治療		シスプラチン ビンデシン マイトマイシン 同時放射線治療	手術±シスプラチン，ビンデシンによる術前化学療法
患者数		160	62
施設数		27	18
c-stage	IIIA/IIIB(%)	29/71	98/2
	N0～1/N2/N3(%)	12/54/34	0/98/2
生存率	2～年(%)	35	36
	3～年(%)	22	25
	5～年(%)	16	17

* Chemoradiotherapy for stage III NSCLC.

** Hidehiro HARADA, M.D., Yuko SHIMMYO, M.D. & Yuichiro OHE, M.D.: 国立がんセンター中央病院肺内科〔〒104-0045 東京都中央区築地5-1-1〕; Department of Internal Medicine, National Cancer Center Hospital, Tokyo 104-0045, JAPAN

表2　放射線化学療法の逐次併用対同時併用の無作為化試験

Author	治　療	n	MST	2年生存率	4年生存率	p-value
Furuse[3]	CDDP+VDS+MMC Sequential TRT	158	13.3m	27.4%	8.9% (5年)	$p=0.039$
	CDDP+VDS+MMC Concurrent TRT	156	16.5m	34.6%	15.8% (5年)	
Curran[9]	CDDP+VBL Sequential TRT		14.6m	32%	12%	—
	CDDP+VBL Concurrent TRT	610 (total)	17.0m	35%	21%	$p=0.046$
	CDDP+ETOP Concurrent TRT (twice daily)		15.2m	34%	17%	$p=0.296$
Fournel[11]	CDDP+VNR Sequential TRT	101	14.5m	26%	14%	$p=0.24$
	CDDP+ETOP Concurrent TRT f/b CDDP+VNR	100	16.3m	39%	21%	
Zatloukal[12]	CDDP+VNR Sequential TRT	50	12.9m	14.3%	9.5% (3年)	$p=0.023$
	CDDP+VNR Concurrent TRT	52	16.6m	34.2%	18.6% (3年)	

CDDP：cisplatin, VDS：vindesine, MMC：mytomycin, VBL：vinblastine, ETOP：etoposide, VNR：vinorelbine, TRT：thoracic radiotherapy

とが知られている．さらに，局所進行非小細胞肺がんに対しては，シスプラチンを含めた化学療法と放射線治療とを併用することで，約15%の根治が得られている[1]．局所進行非小細胞肺がんに対して化学療法ならびに放射線治療を行うことの意義は確立されているが，放射線化学療法の詳細に関してはコンセンサスに至っていないのが現状である．

放射線化学療法の対象患者

ⅢA期と同葉肺転移，胸膜播種，心嚢水，胸水を有しないⅢB期の非小細胞肺がんが放射線化学療法の対象である．ⅢA期の非小細胞肺がんに対し，導入療法に続く手術の適応となる症例はきわめて限られている．病理学的に証明された縦隔リンパ節転移陽性非小細胞肺がんに対する導入化学放射線治療後に手術を行う群と，放射線治療単独群とを比較した第Ⅲ相試験では，手術を行っても長期生存率と無増悪期間の改善を認めなかった[2]．また，切除不能局所進行非小細胞肺がんに対する放射線化学療法同時併用は，切除可能N2非小細胞肺がんに対する手術とほぼ同様の成績が報告されている(表1)[3][4]．したがって，縦隔鏡などで病理学的に縦隔リンパ節転移が確認された症例は，放射線化学療法の適応と考えられる．

放射線治療の適応を検討する際には，照射野が病巣の反対側に及ばないこと(対側肺門リンパ節転移がないこと)と片側肺1/2を超えないことを確認しなくてはならない．放射線治療のもっとも重篤な合併症として放射線肺臓炎があるが，胸部単純写真にて判別できるような肺の線維化を認める場合には，放射線肺臓炎による死亡率が高くなるため放射線治療は避けるべきである[5][6]．

化学放射線治療対放射線単独治療あるいは化学療法単独

11の無作為化試験の1,780症例のデータを用いたメタアナリシスの結果では，シスプラチンを含んだ放射線化学療法の生存は放射線単独療法

を有意に上回っていた[7]．その他のメタアナリシスでも，切除不能の局所進行非小細胞肺がんに対し，放射線治療単独治療群と放射線化学療法群を比較し，放射線化学療法治療群でより高い生存率を認めた．一方，Kubotaらは局所進行非小細胞肺がんに対する放射線化学療法は化学療法単独と比較して2年，3年生存率を有意に改善させたと報告している．また，Sculierらは局所進行切除不能非小細胞肺がんに対して，導入化学療法に奏効した症例を対象に，地固め療法として化学療法を行う群と胸部放射線治療を行う群との第Ⅲ相比較試験の結果を報告している[8]．この試験では放射線治療群は化学療法群と比較し，生存の改善は認められなかったが，放射線治療は長期の局所制御に貢献していることが示唆された．

以上から，化学療法もしくは胸部放射線治療単独による治療は適切ではなく両者の併用が，切除不能の局所進行非小細胞肺がんに対する標準治療として考えられるようになった．

化学療法と放射線治療のタイミング

Japan Clinical Oncology Group(JCOG)とRadiation Therapy Oncology Group(RTOG)による第Ⅲ相試験によって，放射線化学療法の逐次併用と同時併用についての検討がなされている(表2)[3][9]．JCOG9202では320名の切除不能局所進行非小細胞肺がん患者を，シスプチン，ビンデシン，マイトマイシンに続く放射線治療の逐次併用群と同時に放射線治療を行う同時併用群に分け比較した．奏効率は，逐次併用群(66%)に比べ同時併用群(84%)で有意に高かった(p=0.002)．生存期間中央値も逐次併用群(13.3か月)と比較すると，同時併用群(16.5か月)の方が長かった(p=0.039)．2年，3年，4年，5年生存率も同時併用群ではそれぞれ34.6%，22.3%，16.9%，15.8%であり，逐次併用群ではそれぞれ27.4%，14.7%，10.1%，8.9%であった．同時併用群の方が逐次併用群より生存の延長と高い奏効率を示した[3]．RTOGでも同様な結果が報告されており，同時併用群で生存時間中央値17.0か月，4年生存率21%であったのに対し逐次併用群では，それぞれ14.6か月と12%であった(p=0.046)．これらの報告により，骨髄抑制や食道炎などの急性毒性は逐次併用群よりも同時併用群で増強していたものの，シスプチンを用いた化学療法と胸部放射線治療の同時併用療法は逐次併用群と比較し有意に生存を延長していることが示された[9]．

しかし，これらの臨床試験ではシスプラチン＋ビンデシン＋マイトマイシンあるいは，シスプラチン＋ビンプラスチンなどの前世代の併用化学療法が使用されており，試験結果を一般化するには多少の問題があり注意が必要である[3][9]．1990年代には，新しくイリノテカン，パクリタキセル，ドセタキセル，ゲムシタビン，ビノレルビンなどのいわゆる第3世代抗がん剤が開発された．Ⅳ期の非小細胞肺がんに対する化学療法単独治療の場合，プラチナ製剤とこれらの第3世代抗がん剤を組み合わせた2剤併用療法は，前世代の化学療法のレジメンよりも高い効果を認めているが，Ⅲ期非小細胞肺がんを対象に放射線治療併用でこれらの化学療法を比較した成績は報告されていない[10]．とくに，1990年代に開発された第3世代抗がん剤を放射線治療と同時併用する場合には，毒性のために化学療法を減量しなければならないことが大きな問題である．フランスにおける第Ⅲ相試験では切除不能な非小細胞肺がんに対し，放射線化学療法逐次併用群と同時併用群とを比較している[11]．逐次併用群は，シスプラチン＋ビノレルビンを3サイクル行った後に放射線治療を行った．同時併用群は2サイクルのシスプラチン＋エトポシドと胸部放射線同時併用療法を行ったのちにシスプラチン＋ビノレルビンを2サイクル行った．205名がこの試験に登録されており，逐次併用群の生存期間中央値は14.5か月であったのに対し同時併用群では16.3か月であった．2年生存率もそれぞれ26%と39%であった．統計的に有意差はみられなかったが，同時併用群がより好ましい傾向にあった(p=0.24)．Zatloukalらはシスプラチン＋ビノレルビンに放射線治療を逐次併用または同時併用を比較した無作為化試験の結果を報告している[12]．同時併用はより高い奏効率が認められ，逐次併用群よりも生存や無増悪期間においても優れていた．しかし，この試験ではビノレルビンの投与量は両群とも減量されていた．Full-doseの前世代抗がん剤と減量した第3世代抗がん剤

表3　切除不能の非小細胞肺がんに対する放射線治療の1日1回照射対1日数回照射の比較試験

Author	化学療法	放射線治療	*n*	MST (m)	2年生存率 (%)	5年生存率 (%)	*p*-values
Sause[13]	None	2 Gy/day, 60Gy, 5 days/week, Continuous	163	11.4	21	5	—
	CDDP+VBL×2 induction	2 Gy/day, 60Gy, 5 days/week, Continuous	164	13.2	32	8	$p=0.04$
	None	1.2Gy×2/day, 69.6 Gy, 5 days/week, Continuous (HFRT)	163	12.0	24	6	NR
Schild[14]	CDDP+ETOP×2 concurrent	2 Gy/day, 60Gy, 5 days/week, Continuous	117	14	37	13	$p=0.4$
	CDDP+ETOP×2 concurrent	1.5Gy×2/day, 60 Gy, 5 days/week, split (AHFRT)	117	15	40	20	
Saunders[15]	None	2 Gy/day, 60Gy, 5 days/week, Continuous	225	NR	20	NR	$p=0.004$
	None	1.5Gy×3/day, 54 Gy, 7 days/week, Continuous (CHART)	338	NR	29	NR	
Belani[16]	CBDCA+PTX×2 induction	2 Gy/day, 64Gy, 5 days/week, Continuous	56	14.9	34	NR	$p=0.28$
	CBDCA+PTX×2 induction	1.5-1.8-1.5Gy/day, 57.6Gy, 5 days/week, Continuous (HART)	56	20.3	44	NR	

NR：not reported, CDDP：cisplatin, VBL：vinblastine, ETOP：etoposide, CBDCA：carboplatin, PTX：paclitaxel, HFRT：hyperfractionated radiotherapy, AHFRT：accelerated hyperfractionated radiotherapy, CHART：continuous hyperfractionated accelerated radiotherapy, HART：hyperfractionated accelerated radiation therapy

にそれぞれ放射線治療を同時併用した場合の比較試験は報告されていない．

放射線治療のスケジュール

非小細胞肺がんに対する放射線治療は，月曜から金曜まで週5日，合計60～70Gyの照射を6～8週にわたって実施するのが一般的であるが，放射線の多分割照射によって効果を高めることが試みられている（表3）．Hyperfractionated radiotherapy（HFRT）はその一つで，1回の照射量を抑えながら全照射量を増やすことによって，晩期毒性を増加させることなく局所制御を高めることを目標としている．RTOGでは，1回1.2Gyを1日2回施行し，計69.6Gy照射によるHFRTの第Ⅲ相試験を実施したが，この照射法を用いても，従来の1日1回照射を上回る成績を得ることはなかった[13]．Schildらは，化学療法と同時併用したaccelerated hyperfractionated radiotherapy（AHFRT：1回1.5Gy, 1日2回，計60Gy）とstandard radiotherapy（STDRT：1回2 Gy, 1日1回，計60Gy）とを比較した結果を報告しているが，AHFRTとSTDRTの毒性，腫瘍縮小効果，生存はほぼ同等であった[14]．JCOGの6つの臨床試験のデータからAHFRTとSTDRTの結果をretrospective